

DEVELOPMENT OF MULTIPOINT MULTIFREQUENCY POWER SYSTEMS

A Dissertation

by

BABAK RAHROVI

Submitted to the Graduate and Professional School of
Texas A&M University
in partial fulfillment of the requirements for the degree of

DOCTOR OF PHILOSOPHY

Chair of Committee,	Mehrdad Ehsani
Committee Members,	Chanan Singh
	Lazlo B. Kish
	Won-Jong Kim
Head of Department,	Aniruddha Datta

December 2021

Major Subject: Electrical Engineering

Copyright 2021 Babak Rahrovi

ABSTRACT

With increasing the penetration of renewable energy sources and energy storage devices in the power grid, and according to the recent fast-growing trends in electrification of the transportation in land, sea and air vehicles, power electronics converters are becoming one of the dominate parts of the power grids and vehicular power systems. In a power electronics rich power system, there are several power electronics converters that send and receive power bidirectionally and interact with each other. Because of the interactions between power electronics converters, and the need for transferring power bidirectionally, power flow management in smart grids and vehicular power systems is challenging and, in some cases, impossible using conventional power distribution systems. In this research, a novel power distribution system is introduced, which creates the possibility of adding virtual frequency channels to the power system each one of these channels is inherently isolated. The frequency channels will not interfere with each other due to orthogonality of the waveforms, and because of that, power can be transferred between every combination of the sources and loads without interfering others through isolated frequency channels. This power distribution system is based on a multi-frequency multi-port power conversion system in which power is integrated at various frequencies at the source ends and selectively picked up by the loads, or vice versa. In this research, after introducing multiport power conversion systems and their challenges, the concept of the multi-frequency power transfer will be investigated, and finally, the realization and

implementation of the multi-frequency multiport power conversion systems will be discussed. The proof-of-concept will be validated both by both simulation and experiment.

ACKNOWLEDGEMENTS

First and foremost, I am extremely grateful to my supervisor, Prof. Mehrdad Ehsani for his invaluable advice, continuous support, and patience during my PhD study. His immense knowledge and plentiful experience have encouraged me in all the time of my academic research and daily life. I would also like to thank my committee Prof. Chanan Singh, Prof. Laszlo Kish, and Prof. Won-Jong Kim. Finally, I would like to express my gratitude to my parents, my sister, and my brother. Without their tremendous understanding and encouragement in the past few years, it would be impossible for me to complete my study.

TABLE OF CONTENTS

	Page
ABSTRACT	ii
ACKNOWLEDGEMENTS	iv
TABLE OF CONTENTS	v
LIST OF FIGURES.....	vii
LIST OF TABLES	x
CHAPTER I INTRODUCTION	1
CHAPTER II POWER ELECTRONICS RICH POWER SYSTEMS	5
CHAPTER III MULTI ACTIVE BRIDGE POWER CONVERSION SYSTEMS AND THEIR CHALLENGES	9
Dual Active Bridge Converter.....	9
Multi Active Bridge Converter	14
Multi Active Bridge Power Conversion Systems Challenges.....	20
CHAPTER IV MULTI-FREQUENCY POWER TRANSFER CONCEPT IN MULTI PORT POWER CONVERSION SYSTEMS	28
Concept of Multi-Frequency Power Transfer	28
Concept of Multi-Frequency Power Conversion Systems	34
CHAPTER V MULTI-FREQUENCY MULTI ACTIVE BRIDGE POWER CONVERSION SYSTEMS	48
Realization of Multi-Frequency Power Transfer in Dual Active Bridge Converter	48
Multi-Frequency Multi-Phase Multi Active Bridge Power Conversion System	53
Multi-Frequency Triple Active Bridge Power Conversion System.....	58
CHAPTER VI SIMULATION AND EXPERIMENTAL VALIDATION	66
Simulation of Multi-Frequency Triple Active Bridge Power Conversion System	66
Experimental Validation of Multi-Frequency Triple Active Bridge Power Conversion System.....	80

CHAPTER VII CONCLUSION	90
REFERENCES.....	93

LIST OF FIGURES

	Page
Figure 1 Power Electronics Rich Power Systems: (a) DC Micro Grid [22] (b) More Electric Aircraft DC Power System [21] (c) Electric Ship DC Power System [23] (d) Electric Vehicle Charging Infrastructure and Power System [24]	5
Figure 2 More Electric Aircraft DC Power Distribution System.....	7
Figure 3 Power Transfer between Two Sinusoidal Voltages.....	9
Figure 4 A Schematic of a Two Ports DC-DC Converter with AC Link.....	10
Figure 5 Dual Active Bridge Converter	10
Figure 6 Dual Active Bridge Converter Voltage and Current Waveforms [25]	12
Figure 7 Multi Active Bridge Converter (a) Schematic (b) Circuit	14
Figure 8 Star Circuit Model of Multi Active Bridge Converter.....	15
Figure 9 Delta Circuit Model of Multi Active Bridge Converter.....	16
Figure 10 Triple Active Bridge Converter	20
Figure 11 Circuit Model of Triple Active Bridge Converter (a) Star (b) Delta	21
Figure 12 Different Source and Load Combinations in Three-Port Converters	23
Figure 13 Average Power vs Frequency Ratio k Between Two Sinusoidal Voltages with Zero Phase Shifts	32
Figure 14 A Schematic of Multi-Frequency Multiport Power Systems.....	34
Figure 15 Circuit Model of Multi-Frequency Multiport Power Systems with Square-Wave Voltage Sources.....	34
Figure 16 Circuit Model of Multi-Frequency Four-Port Power System with Two Ports in the Primary Side and Two Ports in the Secondary Side	40
Figure 17 Multi-Frequency Multi-Phase Dual Active Bridge (a) Converter (b) Circuit Model.....	49
Figure 18 Multi-Frequency Multi-Phase Multi Active Bridge Power Conversion System.....	53

Figure 19 MFMP MAB Power Conversion System Multi-Winding Transformer in the AC link: (a) Schematic (b) Star Circuit Model (c) Delta Circuit Model.....	54
Figure 20 Multi-Frequency Multi-Phase Triple Active Bridge Power Conversion System with Three-Winding Transformer in AC Link.....	58
Figure 21 Transferring Power Modes in Multi Frequency Multi-Phase Triple Active Bridge Power Conversion System with Three-Winding Transformer in the AC Link.....	59
Figure 22 Load Power vs Phase Shift in a One Source/ Two Loads Multi-Frequency Triple Active Bridge Power Conversion System (a) Load Port 2 (b) Load Port 3.....	62
Figure 23 Averaged Transferred Power vs Phase Shift in a Two Sources/ One Load Multi-Frequency Triple Active Bridge Power Conversion System (a) Source Port 1 (b) Load Port 2 (c) Source Port 3.....	63
Figure 24 Averaged Transferred Power vs Phase Shift in a Two Sources/ One Load Multi-Frequency Triple Active Bridge Power Conversion System with 25% Drop in the Source Voltage 3 (a) Source Port 1 (b) Load Port 2 (c) Source Port 3.....	65
Figure 25 Multi-Frequency Triple Active Bridge Power Conversion System.....	66
Figure 26 AC Voltages in One Source/ Two Loads.....	68
Figure 27 Load Port 2 DC Voltage, and DC Currents in One Source / Two Loads: (a) Resistive Load Port DC Voltage (b) DC Currents.....	68
Figure 28 Linking Transferred Power and Port Power in One Source/ Two Loads: (a) Linking Transferred Power (b) Port Power.....	69
Figure 29 AC Voltages in Two Sources/ One Load.....	71
Figure 30 Load Port 2 DC Voltage, and DC Currents in Two Sources / One Load: (a) Resistive Load Port DC Voltage (b) DC Currents.....	71
Figure 31 Linking Transferred Power and Port Power in Two Sources/ One Load: (a) Linking Transferred Power (b) Port Power.....	72
Figure 32 AC Voltages in Two Sources/ One Load with 25% Voltage Drop in Source Port 3.....	74

Figure 33 Load Port 2 DC Voltage, and DC Currents in Two Sources / One Load with 25% Voltage Drop in Source Port 3: (a) Resistive Load Port DC Voltage (b) DC Currents	74
Figure 34 Linking Transferred Power and Port Power in Two Sources/ One Load with 25% Voltage Drop in Source Port 3: (a) Linking Transferred Power (b) Port Power	75
Figure 35 AC Voltages in One Source/ One Load/ One Port with Zero Power	77
Figure 36 DC Voltages, and DC Currents in One Source/ One Load/ One Port with Zero Power: (a) Port 2 and Port 3 DC Voltage (b) DC Currents.....	77
Figure 37 Linking Transferred Power and Port Power in One Source/ One Load/ One Port with Zero Power: (a) Linking Transferred Power (b) Port Power	78
Figure 38 Multi-Frequency Triple Active Bridge Power Conversion System Experimental Setup.....	80
Figure 39 Experimental Results for One Source/ Two Loads with Balanced Loads.....	82
Figure 40 Experimental Results for One Source/ Two Loads	84
Figure 41 Experimental Results for Two Sources/ One Load	85
Figure 42 Experimental Results for Two Sources/ One Load with Voltage Drop in One Source and Load Power of 19.2 W	87
Figure 43 Experimental Results for One Source/ One Load/ One Port with Zero Power	88

LIST OF TABLES

	Page
Table 1 More Electric Aircraft Power System Specification	62
Table 2 Operation Condition in Simulated One Source/ Two loads System	67
Table 3 Operation Condition in Simulated Two Sources/ One Load System.....	70
Table 4 Operation Condition in Simulated Two Sources/ One Load System with a Voltage Drop in One of the Source Ports	73
Table 5 Operation Condition in the Simulated System with One Source/ One Load/ One Port with Zero Power	76
Table 6 Experiment Condition for One Source/ Two Loads with Balanced Loads.....	82
Table 7 Experiment Condition for One Source/ Two Loads with Unbalanced Loads	83
Table 8 Experiment Condition for Two Sources/ One Load	85
Table 9 Experiment Condition for Two Sources/ One Load	86
Table 10 Experiment Condition for One Sources/ One Load/ One Port with Zero Power	88

CHAPTER I

INTRODUCTION

Last two decades have introduced a paradigm shift for power systems. Dense loads, such as the internet data centers, and dispersed loads, such as electric vehicles, have kept growing in the major cities. In addition, with the growing threat of climate catastrophe and the shortage of oil resources, it is becoming more urgent to transition away from fossil fuel-based electricity and to increase the penetration of renewable power sources and energy storages into the power system. Furthermore, the liberalization of energy markets has caused a high level of regional interconnection through which the consumers can interchange power with the grid which needs a high-quality power management system between different power sources and loads. On the other hand, electrification of the transportation is becoming one of the most promising solutions to make the transition from fossil fuel-based transportations, and it is expanding to all kinds of vehicles in land, sea and air. To interconnect the new sources of power to the grid, or to transfer power between different sources and loads, bidirectionally, in vehicular power systems, several power electronics converters are required each one of which interact with one another. Therefore, power flow management in smart grids, and in mobile power systems is a challenging issue which needs to be addressed.

To interconnect different power electronics converters in a system, one strategy is to employ multiple individual power converters. However, it presents an increased number of components, communication links, and power stages. An alternative is to integrate the individual power converters into one and making a multiport power conversion system.

Various multi-port converter solutions have been reported in [1]-[12] for different applications ranging from solid-state transformers to electric vehicles and more electric aircraft. The major challenge in these systems is the interactions between the ports and not having flexibility in power flow management between all sources and loads. These issues get more complicated when there are unbalanced load demands, unequal source voltages, limitation in supplying power, or failures in one or more ports.

One approach to address these challenges is to use time-sharing techniques to minimize the interaction among multiple sources of the system [13]. However, this scheme is employed only between the source ports, and by using these techniques, only one source can transfer power to the load at a time, which avoids simultaneous power transfer between different sources and loads and limits the power rating of the system. In another approach, a dual transformer based three-port converter is reported to address asymmetrical sources [14]-[15]. However, this configuration does not have the flexibility to transfer power bidirectionally between any selected ports, because of not having a linking inductance between the source ports. In addition, with increasing the number of ports, the number of transformers is increased, and the flexibility in power management is decreased. An alternative is reported in [16]-[17] for hybrid AC-DC power systems. In this technique, the DC power is superposed onto the AC one and transmitted simultaneously over the same line. Another approach is to get help from orthogonality of the signals with different frequencies. The use of multiple frequencies for signal transmission is a well-established technique in the radio communication and television broadcasting systems. However, the use of multiple frequencies for transferring electrical power did not receive

a notable attention. Only few studies employed the principal of orthogonal power flow to address some challenges. [18] used this principal to overcome the problem of charge balance on the submodule capacitors in modular multi-level converters. [19] explored the possibility of ac bus voltage and current waveform shaping in single-phase, small-scale islanded grids by superposition of odd harmonic frequencies.

In this research, a novel power electronics-based power distribution system is introduced, which creates the possibility of adding virtual frequency channels to the power system each one of these channels is inherently isolated. The frequency channels will not interfere with each other due to orthogonality of the waveforms. All the harmonic frequencies from the power electronics converters are included in the system, and because of that, the frequency channels are completely decoupled, and power can be transferred between every combination of the sources and loads, independently through isolated frequency channels, without interfering the others. The proposed system is based on a multi-frequency multiport power conversion system in which power is integrated at various frequencies at the source ends and selectively picked up by the loads, or vice versa. The multi-frequency multiport power conversion system, introduced in this research, is based on Dual Active Bridge (DAB) converters because of having galvanic isolation and bidirectional power transfer capability [20]. In order to make a multiport power conversion system using DAB, several converters can be integrated into one to make what is called Multiple Active Bridge (MAB) power conversion system. Using MAB, the overall power density of the system is increased and the communication, synchronization, control, and the ability to interchange power among different ports of the system is easier. However, it

increases the control complexity, and the design of the converter would be much more challenging [21].

In this research, after an introduction of power electronics rich power systems in Chapter II, the dual active bridge and multiple active bridge converters will be introduced in Chapter III, and the motivations of transferring power through isolated frequency channels in multiport power conversion systems will be discussed in this chapter. Then, the concept of transferring power through multiple frequency channels, will be investigated in Chapter IV, and this concept will be discussed for multiport power conversion systems in the same chapter. Finally, the concept of multi-frequency power transfer will be realized in multi-frequency multi-active-bridge power conversion systems in Chapter V, and a multi-frequency Triple Active Bridge will be validated through simulation and experiment in Chapter VI.

CHAPTER II

POWER ELECTRONICS RICH POWER SYSTEMS

A power electronics rich power system is a system in which different AC and DC loads and sources are interconnected through different power electronics converters. It can be a smart grid or an on-board power system. Some examples of power electronics rich power systems are shown in Fig. 1.

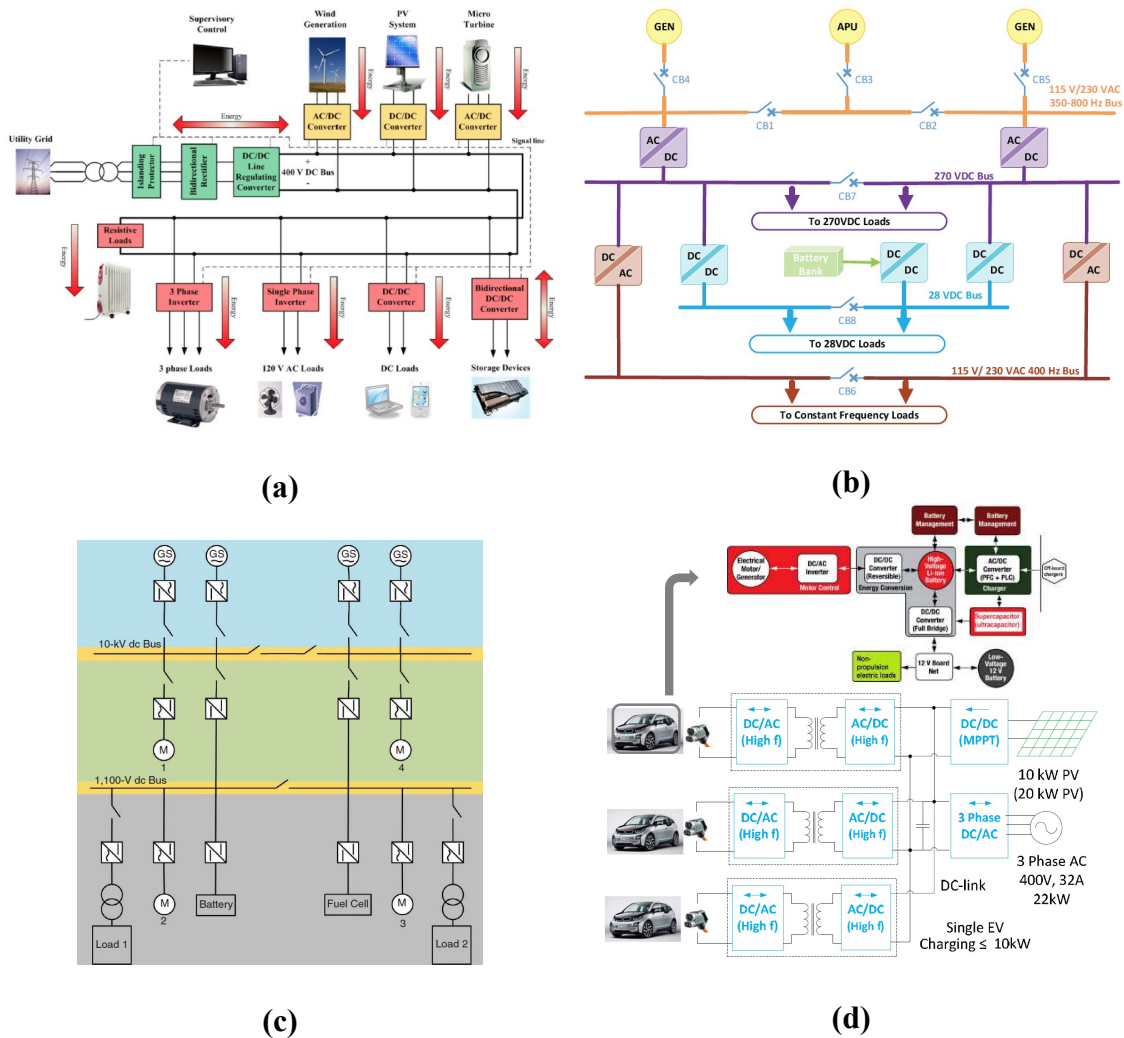


Figure 1 Power Electronics Rich Power Systems: (a) DC Micro Grid [22] (b) More Electric Aircraft DC Power System [21] (c) Electric Ship DC Power System [23] (d) Electric Vehicle Charging Infrastructure and Power System [24]

In this research, More Electric Aircraft (MEA) power system is selected as the representative of power electronics rich power systems to be discussed in more detail.

In MEA, the hydraulic and mechanical components of the aircraft are replaced with their electrical counterparts which results in reducing mass, fuel consumption and environmental impact, as well as higher capability of power and energy management. In MEA, engine is responsible for providing thrust and for driving generator shafts. As it is shown in Fig. 1b, the MEA electrical power is provided by integrated starter generators. There is also an auxiliary power unit which is responsible for supplying power when the aircraft is on the ground and while the aircraft is under certain conditions, such as emergencies. Batteries are responsible for providing the transient power of the loads, capturing the regenerative power, supplying emergency power, providing the additional power to balance the rectified dc power from the engine-driven ac generators and assisting in supplying power for starting engine.

To distribute power in MEA, there are three architectures: constant frequency, variable frequency and DC distribution in which the DC distribution architecture is getting more attentions recently. Because, making coupling between the main source and the storage devices is easier in this architecture and the overall mass of the power distribution network is lower than the other architectures. In addition, it is a better option when skin effects in conductors is an issue, and when increasing the number of energy storage devices is required in the future. Moreover, a dc system needs only two cables to transport power which leads to a decrease in the number of power converters and the required cable insulation [21].

Fig. 1b, shows a schematic of the MEA DC power distribution system. As can be seen from this figure, the distributed DC voltage in this architecture is provided by two AC/DC rectifiers that convert the variable frequency voltage of the generator output to a DC voltage at the 270 VDC busbar. Then, this 270 VDC voltage is converted to a 28 VDC using two DC-DC converters to supply DC loads, and to a 230 VAC to supply AC loads. Also, there is a battery in the system to start the generators and to supply DC loads when it is needed. The voltage of the battery is usually 135 V and can be a different value according to the type of the aircraft. To interconnect the 270 VDC busbars, 28 VDC busbars and the battery, one strategy is to employ multiple individual DC-DC power converters. However, it presents an increased number of components, communication links, and power stages. Another alternative is to integrate the individual power converters into one and making a multiport power conversion system, as it is shown in Fig. 2.

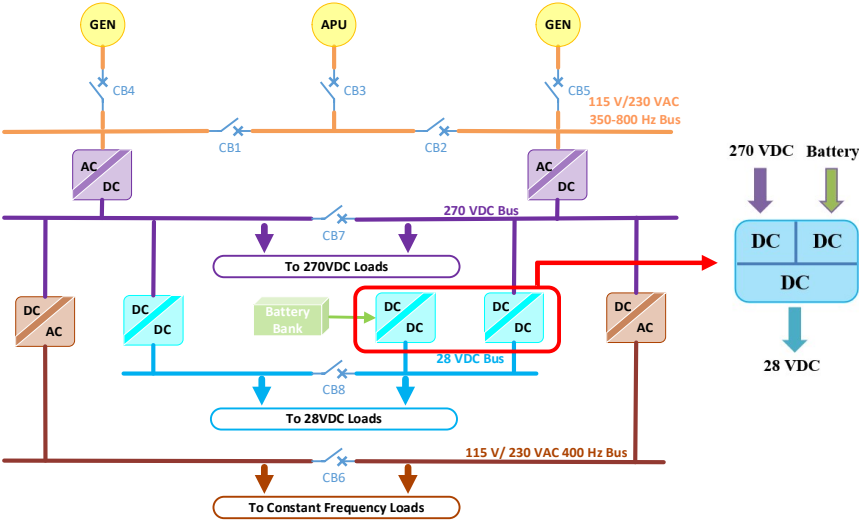


Figure 2 More Electric Aircraft DC Power Distribution System

The multiport converter in Fig. 2 is a three ports converter, which is the result of integrating two individual DC-DC converters. As can be seen from the figure, the three ports converter has one 270 VDC port from the generator rectifier, one 28 VDC port to supply DC loads and one 135 VDC port for connecting to the battery. Although this configuration increases the complexity of the design, it can reduce the number of components and increase the power management capability of the system.

Having a galvanic isolation between the ports in DC-DC power converters in high power applications with different voltage levels such as MEA power system is necessary. There are several types of DC-DC converters with galvanic isolation in the literature [21] in which Dual Active Bridge (DAB) is the most promising candidate for high power applications because of its bidirectional power transfer capability without a significant increase in the control complexity [20]. By integrating several DAB converters into one and making a Multiple Active Bridge (MAB) power conversion system the overall power density and the flexibility to interchange power among different ports of the system can be increased [21]. MAB power conversion systems and their challenges will be discussed in the next chapter.

CHAPTER III
MULTI ACTIVE BRIDGE POWER CONVERSION SYSTEMS AND THEIR
CHALLENGES

Dual Active Bridge Converter

In order to analyze a multiport power conversion system, first the concept of power transfer in a two ports system should be discussed. It is well known that the net power transferred between two sinusoidal voltage sources, shown in Fig. 3, can be obtained using (1). As can be seen from this equation, the net transferred power between two sinusoidal voltages depends on the rms value of the voltages V_1 and V_2 , frequency of the sinusoidal waveforms f , inductance of the link between the voltages L , and the phase shift angle between the waveforms φ_{12} .

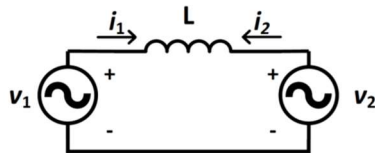


Figure 3 Power Transfer between Two Sinusoidal Voltages

$$P_{12} = \frac{V_{1rms}V_{2rms}}{2\pi fL} \sin\varphi_{12} \quad (1)$$

The sinusoidal voltages are generated using generators in the conventional power systems. In vehicular power systems and the systems including renewable energy sources and energy storage devices, the voltages are generated by power electronics inverters. Fig. 4 shows a schematic of a two ports system including two inverters, a linking inductance and

two DC voltage sources. As can be seen from this figure, the AC side of each inverter is a square wave voltage which maximizes the utilization of the voltage sources and increase the power transfer capability of the system. However, it can be any other modulated waveform but with the cost of a reduction in the power transfer capability.

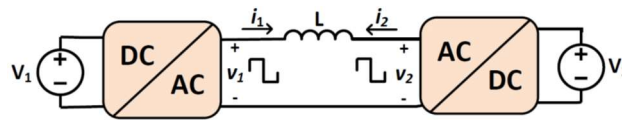


Figure 4 A Schematic of a Two Ports DC-DC Converter with AC Link

The square wave voltages can be realized by using two full bridge inverters, as it is shown in Fig. 5, which is called Dual Active Bridge (DAB) Converter [2].

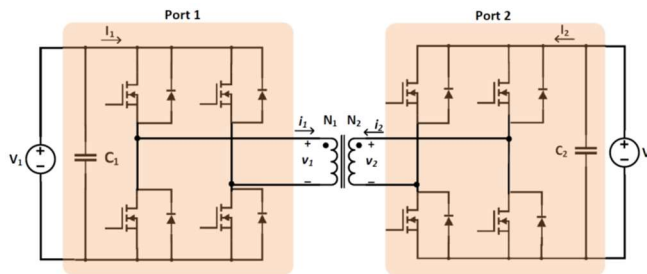


Figure 5 Dual Active Bridge Converter

As can be seen from this figure, the full bridges are linked through an isolation transformer which can be connected in series with an inductor in the AC link. The square wave voltages can be realized by half bridges instead of full bridges as well, with the cost of a reduction in the utilization of the voltage sources to half. Equation (2) shows the net power transferred between the ports in a DAB.

$$P_{12} = \frac{nV_1V_2}{2\pi f_{sw}L} \varphi_{12} \left(1 - \frac{|\varphi_{12}|}{\pi}\right) \quad (2)$$

As can be seen from (2), the power flow between the bridges is determined by the transformer primary and secondary square-wave voltage amplitudes V_1 and V_2 , turns ratio of the transformer $n = N_1/N_2$, the frequency of the waveforms f_{sw} which is the switching frequency of the bridges, the AC link inductance L , and the phase shift between the square-wave voltages φ_{12} . Neglecting the transformer magnetizing inductance and parasitic capacitances, the inductance L in the AC link can be determined by the total leakage inductance of the transformer or by adding an extra inductor in the link [3]. The switching frequency and the AC link inductance need to be determined according to the design requirement of the converter such as size, efficiency, power rating, etc. Conventionally, phase shift is the only parameter that controls the value and the direction of the power flow in this converter as it is shown in (3).

$$\begin{aligned} & \text{if } \varphi_{12} > 0 \ (\varphi_2 < \varphi_1) \text{ then } P_{12} > 0 \text{ and power is transferred from port 1 to port 2} \quad (3) \\ & \text{if } \varphi_{12} < 0 \ (\varphi_2 > \varphi_1) \text{ then } P_{12} < 0 \text{ and power is transferred from port 2 to port 1} \end{aligned}$$

In the most common modulation principle, which is called phase shift modulation, DAB operates with the maximum duty cycle of $D = 1/2$ in both sides. By solely varying the phase shift between $-\pi/2 < \varphi < \pi/2$, the transferred power can be controlled

bidirectionally between the two ports. The maximum power is transferred when $\varphi = \pi/2$ or $-\pi/2$.

Fig. 6 shows the voltages $v_1(t)$, $nv_2(t)$ at the AC side of the converter and the current $i_L(t)$ in the AC link in steady state all referred to the primary side of the transformer for a power flow from port 1 to port 2.

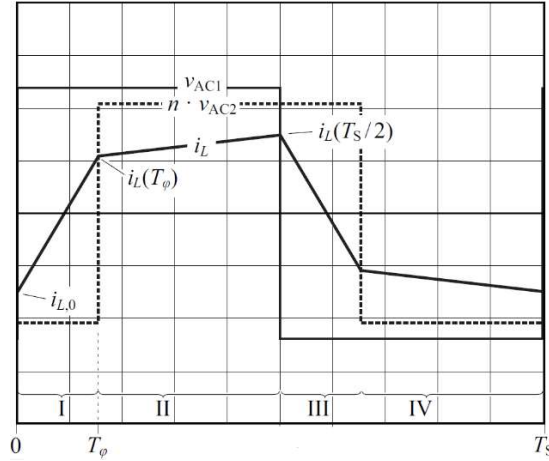


Figure 6 Dual Active Bridge Converter Voltage and Current Waveforms [25]

As can be seen from this figure, the voltage $nv_2(t)$ has a negative phase shift respect to the voltage $v_1(t)$ which leads to a power transferred from port 1 to port 2. The AC link inductor current can be determined using the difference between the $v_1(t)$ and $nv_2(t)$ voltages, as it is shown in (4). Integrating the difference between the voltages $v_1(t)$ and $nv_2(t)$ over the switching frequency results a piece-wise function for $i_L(t)$ which is shown in (5).

$$i_L(t) = i_L(0) + \frac{1}{L} \int_0^{T_s} (v_1(t) - nv_2(t)) dt \quad (4)$$

$$i_L(t) = \begin{cases} i_L(0) + \frac{(V_1 + nV_2)t}{L} & 0 < t < \frac{T_s\varphi}{2\pi} \\ i_L\left(\frac{T_s\varphi}{2\pi}\right) + \frac{(V_1 - nV_2)(t - \frac{T_s\varphi}{2\pi})}{L} & \frac{T_s\varphi}{2\pi} < t < \frac{T_s}{2} \\ i_L\left(\frac{T_s}{2}\right) + \frac{(-V_1 - nV_2)(t - \frac{T_s}{2})}{L} & \frac{T_s}{2} < t < \frac{T_s}{2} + \frac{T_s\varphi}{2\pi} \\ i_L\left(\frac{T_s}{2} + \frac{T_s\varphi}{2\pi}\right) + \frac{(-V_1 + nV_2)(t - \frac{T_s}{2} - \frac{T_s\varphi}{2\pi})}{L} & \frac{T_s}{2} + \frac{T_s\varphi}{2\pi} < t < T_s \end{cases} \quad (5)$$

Where T_s is the time period associated with the switching frequency of f_{sw} . The initial current $i_L(0)$ can be found by: $i_L(0) = -I_{avg}$, where I_{avg} is the average of (5) shown in (6).

$$I_{avg} = \frac{1}{T_s} \int_0^{T_s} i_L(t) dt = \frac{T_s}{L} \left(\frac{V_1}{4} - \frac{nV_2}{2} \left(\frac{-\varphi}{\pi} + \frac{1}{2} \right) \right) \quad (6)$$

This analysis can be expanded to MAB which will be discussed in the next section.

Multi Active Bridge Converter

An N -port MAB converter is comprised of N full-bridge modules magnetically coupled through an N -winding high frequency transformer as illustrated in Fig. 7.

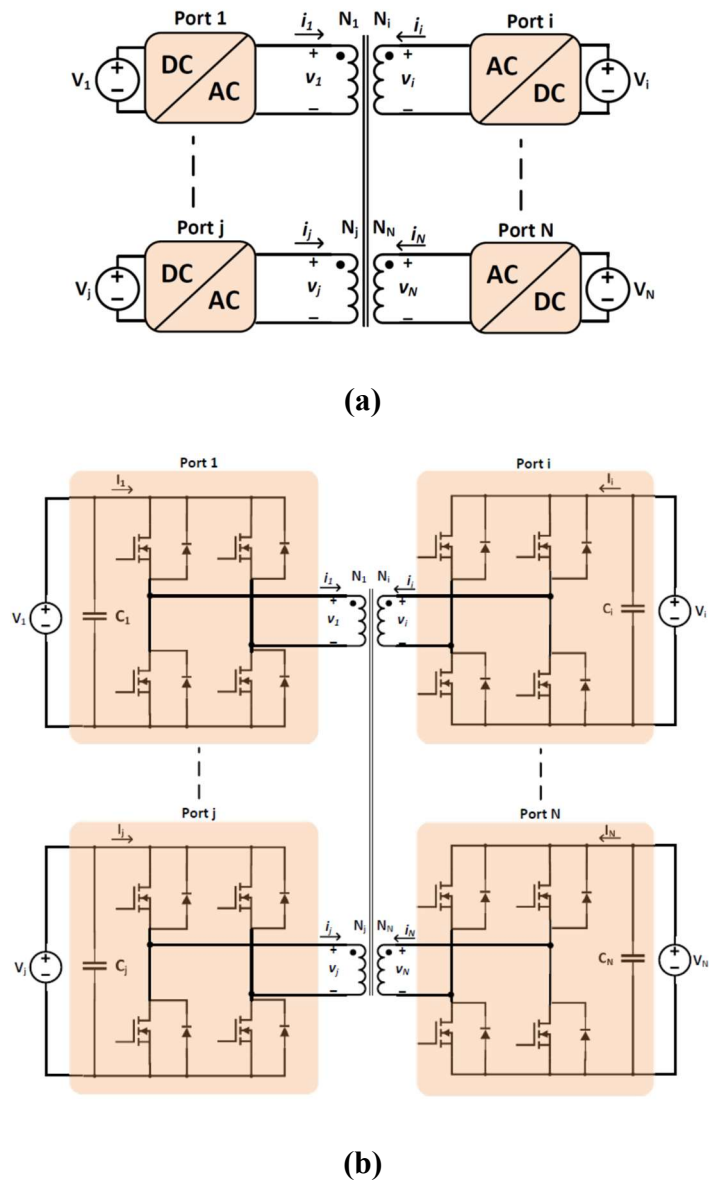


Figure 7 Multi Active Bridge Converter (a) Schematic (b) Circuit

Where for example V_j is the DC voltage in port j , v_j is the voltage in the AC side of port j , i_j is the AC current corresponding to port j , and N_j is the number of turns in the winding corresponds to port j .

The DAB converters can be considered as the simplest version of MAB converters. The equation derived therein for the DAB power transfer can be extended to any MAB converter. In order to derive the equations for the MAB, first, the linking inductance between each two ports must be obtained. To find the linking inductances, the circuit model of the multi-winding transformer must be illustrated, first. The multi-winding transformer in the AC link of the MAB converter can be modeled using the leakage inductances of the transformer windings as it is shown in Fig. 8 [26].

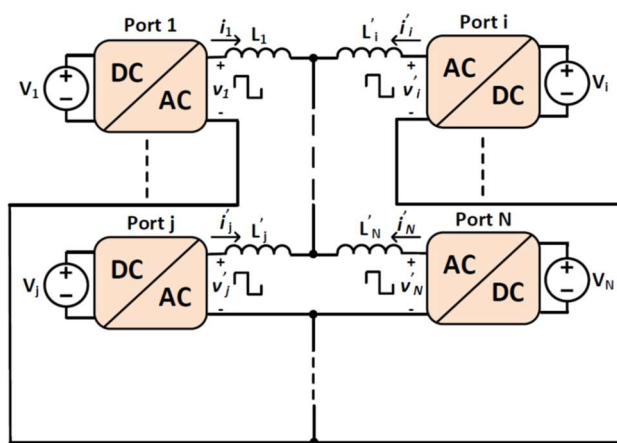


Figure 8 Star Circuit Model of Multi Active Bridge Converter

This figure shows the star circuit model of a MAB converter. The inductor L'_j placed on the AC side of the port j , i.e., represents the effect of the corresponding winding leakage inductance combined with an external inductor (if needed) reflected to port 1. The value

frequency, and L_{ij} is the equivalent inductance between ports i and j in the delta circuit model. The linking inductance L_{ij} can be calculated found by (9) [3].

$$L_{ij} = (L'_i + \left(\sum_{j \neq i}^N \frac{1}{L'_j} \right)^{-1}) (L'_j \sum_{l \neq i, j}^N \frac{1}{L'_l} + 1) \quad (9)$$

The current i'_{ij} in Fig. 9 is the AC current through the link inductor L_{ij} flows from port i to port j . The current i'_i in the AC side of each port is given by (10).

$$i'_i = \sum_{l \neq i}^N i'_{il} \quad (10)$$

The total power in port i can be found by the summation of the powers in the link associated with the port i as it is shown in (11).

$$P_i = \sum_{i \neq j}^N P_{ij} \quad (11)$$

Where P_{ij} can be found by (8).

Also, the summation of the powers in all ports must be zero in a lossless system, as it is shown in (12).

$$\sum_{i=1}^N P_i = 0 \quad (12)$$

Having considered above discussion, it can be seen that there is a link between each one of the ports and all the other ports of the system, which leads to having interactions between all the ports in the system. This limits the flexibility in transferring power between

any selected combination of the ports independently from the others. The issue of independently controlling power flow between each two selected ports of a multiport power conversion system gets more challenging when there are unbalanced load demands, different source voltages, limitations in supplying power, faults in one or more ports, different linking inductance values, or when there are series or parallel connections between the ports. Because, as it is mentioned in the previous sections, conventionally, phase shift is the only parameter to control the transferred power in this system and any changes in the phase angle in each one of the ports results in a change in the power flow in the whole system. Therefore, the phase shift in each port is dependent to the phase shifts in all the other ports, and consequently the transferred power between each two ports is dependent to the power flow between the other ports. For example, if the demanded load power or the source voltage in one of the ports is changed, the transferred power in all the other ports will be changed resulting in an undesired power flow in the system. To address this issue for a system with any number of ports, and for transferring power selectively between any combination of the ports with any source voltages or demanded load powers, a solution is proposed in this research. That is, creating virtual isolated frequency channels between each two ports of the system so that the power can be transferred completely independently through each frequency channel without interfering with the others. In order to discuss the proposed solution, first, the power flow management problem in the conventional multiport power conversion systems must be analyzed in more details. To discuss all the possibilities and recognize the challenges, in this research, a three ports version of the converter called Triple Active Bridge (TAB) is selected to be investigated

in more details. It can be proven that the results of this analysis will be valid for any number of the ports as well.

Multi Active Bridge Power Conversion Systems Challenges

To discuss the MAB power conversion system challenges, the three-port version of the system called Triple Active Bridge converter will be analyzed in this section. TAB is a converter with three full bridges which are coupled through a three winding transformer as it is shown in Fig. 10.

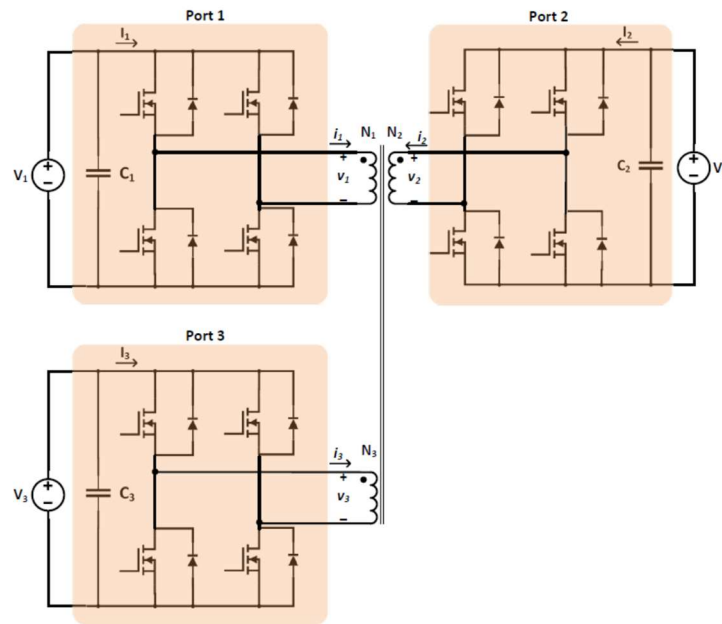


Figure 10 Triple Active Bridge Converter

Where V_1, V_2, V_3 are the DC voltages of the ports 1, 2 and 3; v_1, v_2, v_3 are the voltage in the AC side of the ports 1,2 and 3; i_1, i_2, i_3 are the AC currents corresponding to the ports 1, 2, 3; and N_1, N_2, N_3 are the number of turns in the windings corresponds to the ports 1, 2, 3.

As can be seen from Fig. 10, the windings of the transformer are all coupled and, therefore, power can be transferred, bidirectionally, between any combination of the ports.

According to the previous discussion about the circuit model of a multi-winding transformer, the star and delta circuit model of a TAB converter are as Fig. 11.

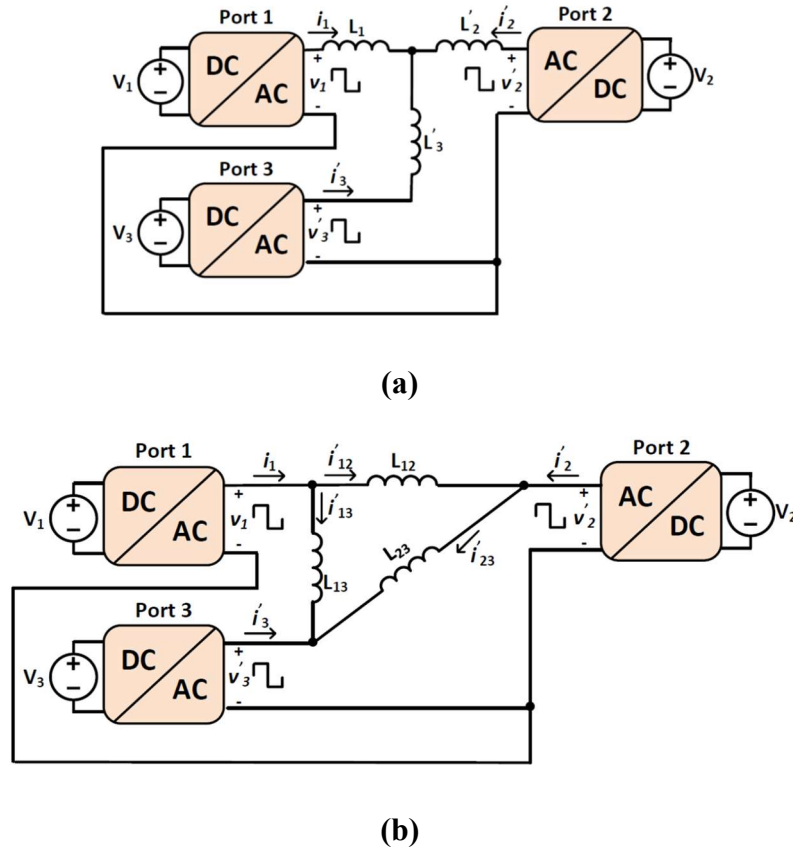


Figure 11 Circuit Model of Triple Active Bridge Converter (a) Star (b) Delta

Where the currents $i_1(t)$, $i'_2(t)$ and $i'_3(t)$ are the currents in the AC side of each port reflected to port 1; the voltages $v_1(t)$, $v'_2(t)$ and $v'_3(t)$ are the voltages in the AC side of each port reflected to port 1; the inductors L_1 , L'_2 and L'_3 in Fig. 11a are the leakage inductances of the transformer windings in each port referred to port 1. Using these leakage inductances and according to (9), the link inductances L_{12} , L_{13} and L_{23} in Fig. 11b can be found by (13).

$$\begin{aligned}
L_{12} &= \frac{L_1 L'_2 + L_1 L'_3 + L'_2 L'_3}{L'_3} \\
L_{13} &= \frac{L_1 L'_2 + L_1 L'_3 + L'_2 L'_3}{L'_2} \\
L_{23} &= \frac{L_1 L'_2 + L_1 L'_3 + L'_2 L'_3}{L_1}
\end{aligned} \tag{13}$$

Also, the currents $i_1(t)$, $i'_2(t)$ and $i'_3(t)$ in Fig. 11a can be calculated by (14).

$$\begin{aligned}
i_1(t) &= i_{12}(t) + i_{13}(t) \\
i'_2(t) &= -i_{12}(t) + i_{23}(t) \\
i'_3(t) &= -i_{13}(t) - i_{23}(t)
\end{aligned} \tag{14}$$

The average power transferred between each two ports can be found by (15).

$$\begin{aligned}
P_{12} &= \frac{(V_1 V'_2)}{2\pi f_{sw} L_{12}} \varphi_{12} \left(1 - \frac{|\varphi_{12}|}{\pi}\right) \\
P_{13} &= \frac{(V_1 V'_3)}{2\pi f_{sw} L_{13}} \varphi_{13} \left(1 - \frac{|\varphi_{13}|}{\pi}\right) \\
P_{23} &= \frac{(V'_2 V'_3)}{2\pi f_{sw} L_{23}} \varphi_{23} \left(1 - \frac{|\varphi_{23}|}{\pi}\right)
\end{aligned} \tag{15}$$

Where

$$\begin{aligned}
V'_2 &= \frac{N_1}{N_2} V_2, V'_3 = \frac{N_1}{N_3} V_3 \\
\varphi_{12} &= \varphi_1 - \varphi_2 \\
\varphi_{13} &= \varphi_1 - \varphi_3 \\
\varphi_{23} &= \varphi_2 - \varphi_3
\end{aligned} \tag{16}$$

And the total average power in each port can be found by (17).

$$\begin{aligned}
P_1 &= P_{12} + P_{13} \\
P_2 &= -P_{12} + P_{23} \\
P_3 &= -P_{13} - P_{23}
\end{aligned} \tag{17}$$

Where $P_1 + P_2 + P_3 = 0$.

For simplicity in analyzing power flow, in this study, it is assumed that $L_1 = L_2 = L_3 = L/3$, and $N_1/N_2 = N_1/N_3 = 1$. Therefore, $L_{12} = L_{13} = L_{23} = L$.

Depending on the number of sources and loads, there could be different modes operation for transferring power between the ports in the system. For a three-port system, there are three possibilities in terms of the number of the sources and loads:

- One source and two loads
- Two sources and one load
- One source, one load, and one port with zero net power

These possibilities are shown in Fig. 12.

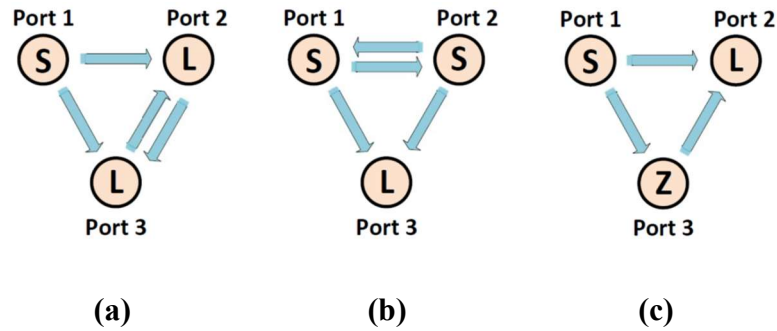


Figure 12 Different Source and Load Combinations in Three-Port Converters

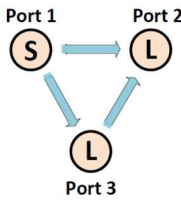
In Fig. 12a, there are one source and two loads in the system. In this mode, port 1 is the source port because of that $\varphi_{12} > 0$ and $\varphi_{13} > 0$. Depending on the value of the phase shifts, there could be a power transferred from port 2 to port 3 or vice versa. However, at the end of the day, both work as a load. In Fig. 12b, there are two sources and one load in the system. In this mode, $\varphi_{13} > 0$ and $\varphi_{23} > 0$ and because of that port 3 works as a load

port. Depending on the value of the phase shifts, there could be a power transferred from port 1 to port 2 or vice versa, but again, at the end of the day, both work as a source port. In Fig. 12c, there is one source, one load, and one port with zero net power in the system. In this mode, $\varphi_{12} > 0$, $\varphi_{13} > 0$, $\varphi_{23} > 0$, and to have zero net power in port 3, the value of the power transferred from port 1 to port 3 must be equal to the value of the power which is transferred from port 3 to port 2.

Below is a summary of all possible modes of transferring power in a three-port power conversion system, in different combinations of sources and loads. This classification is based on the number of sources and loads in the system which is dictated by the system requirement. It can be proven that all other possibilities can be subcategorized under one of these modes.

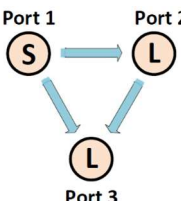
✚ One Source and Two Loads

Mode 1:

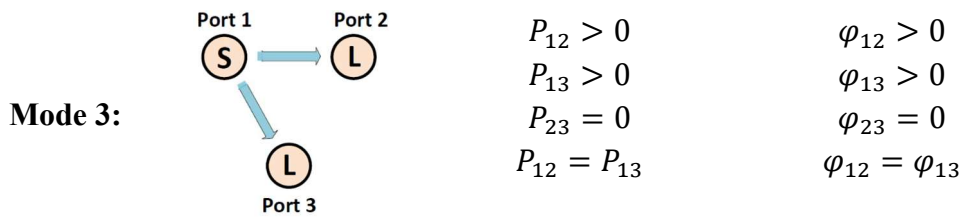


$P_{12} > 0$	$\varphi_{12} > 0$
$P_{13} > 0$	$\varphi_{13} > 0$
$P_{23} < 0$	$\varphi_{23} < 0$
$P_{12} > P_{13}$	$\varphi_{12} > \varphi_{13}$
$P_{13} < P_{23}$	$\varphi_{13} < \varphi_{23}$
$P_{13} - P_{23} = P_{12}$	$\varphi_{13} - \varphi_{23} = \varphi_{12}$

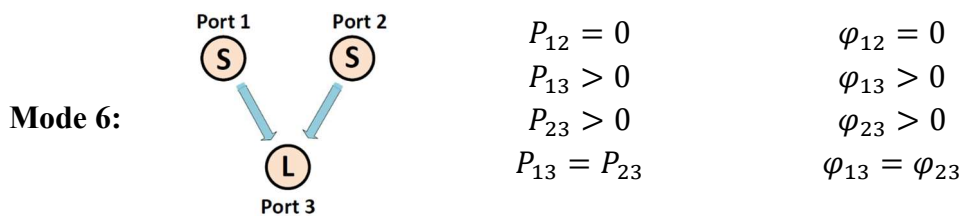
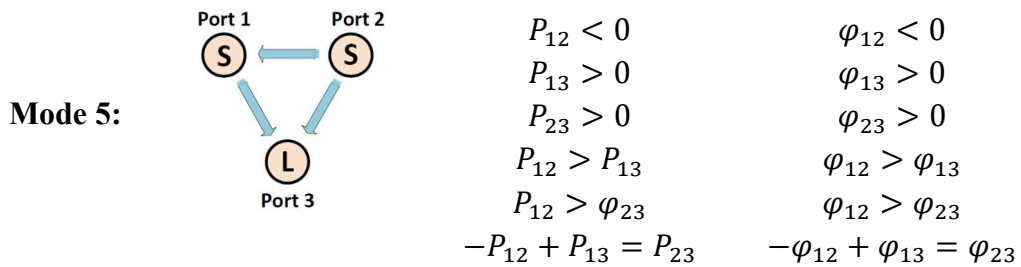
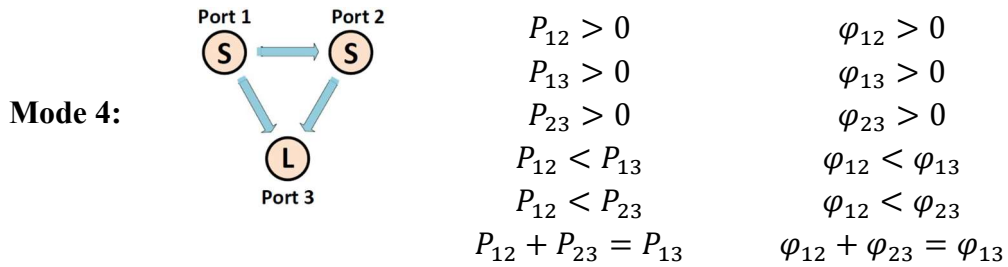
Mode 2:



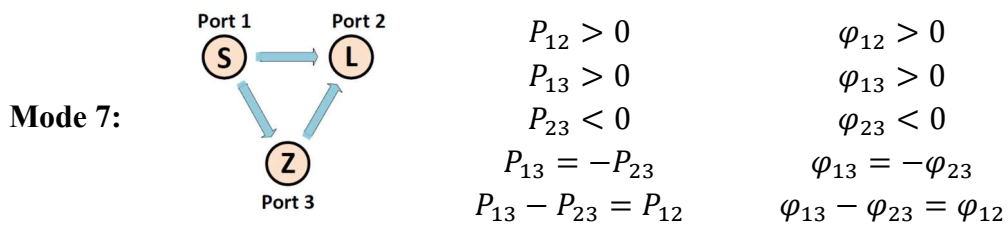
$P_{12} > 0$	$\varphi_{12} > 0$
$P_{13} > 0$	$\varphi_{13} > 0$
$P_{23} > 0$	$\varphi_{23} > 0$
$P_{12} < P_{13}$	$\varphi_{12} < \varphi_{13}$
$P_{12} > P_{23}$	$\varphi_{12} > \varphi_{23}$
$P_{12} + P_{23} = P_{13}$	$\varphi_{12} + \varphi_{23} = \varphi_{13}$



Two Sources and One Load



One Source, One Load, and One Port with Zero Net Power



In Mode 1 and Mode 2, the demanded loads are unbalanced which results to have an undesired power transferred between the load ports. This transferred power between the load ports leads to not being able to independently control the power flow between the source and the load ports. Because, any changes in the demanded power in one of the loads affects the amount of the transferred power on the other one. The only way to avoid this undesired transferred power between the load ports, using conventional phase shift control, is to have a same phase shift in the load ports. However, having a same phase shift between the source and the load ports happens only when there is an equal demanded power in both load ports (Mode 3). Therefore, with unbalanced load demands, the power flow between the load ports is unavoidable using the conventional phase shift method.

There is a same story for the case of two sources and one load with unbalanced voltages in the source ports as it is shown in Mode 4 and Mode 5. In case of having unbalanced voltage sources or if there is a change in the value of the voltage in one of the source ports, there would be an undesired power transferred between the source ports which avoids to having an independent power flow between the ports. The only way to avoid transferring power between the source ports is to have a same phase shift in the source ports. However, having a same phase shift between the sources and the load port happens only when there is a voltage in the source ports which is shown in Mode 6.

Regarding Mode 7, it is desired to transfer power directly from one port, e.g., port 1, to the other, e.g., port 2, without interchanging power in the third port. This cannot be happened when the magnitude of the voltage in port 3 is lower than that of port 1 and/or

port 2 even if all the switches of the full-bridge in port 3 are remaining in the off-state, as the anti-parallel free-wheeling diodes would be forced into conduction by higher output voltages in port 1 and/or port 2 [8]. Therefore, as it is shown in Mode 7, the only way to have zero net power in port 3 is to assign the phase shifts such that the value of the power which is transferred from port 1 to port 3 is equal to the power which is transferred from port 3 to port 2. However, in this case, there would an undesired power transferred from port 1 to port 3 and from port 3 to port 2 which avoids transferring power between the ports independently.

To address these problems and to control the power flow between each two ports of the converter independently, a novel multi frequency multi active bridge power conversion system has been introduced in this research. The objective of the proposed system is to transfer power only between the ports which have a same switching frequency independently from others. To realize this objective and to create an independent channel between each two ports, first, it must be found that under what condition the net transferred power between two phase shifted ports with different frequencies is zero. To answer this question, first, the concept of power transfer in a multi frequency power system must be investigated.

CHAPTER IV
MULTI-FREQUENCY POWER TRANSFER CONCEPT IN MULTI-PORT POWER
CONVERSION SYSTEMS

Concept of Multi-Frequency Power Transfer

In order to analyze a multi frequency power conversion system, the analysis should be started with a system with sinusoidal voltage sources, and then it can be extended to other voltage waveforms like square-waves if the voltages are generated by inverters. Because, according to the Fourier Transform, any waveform can be written by the summation of sinusoids with different amplitudes and frequencies. For example, for a square-wave generated by a full bridge inverter with the switching frequency of f_{sw} , the harmonic content of the waveform is included sinusoids with odd coefficients of the switching frequency: $f_{sw}, 3f_{sw}, 5f_{sw}, 7f_{sw} \dots$ with the amplitude of $4/\pi, 4/3\pi, 4/5\pi, 4/7\pi \dots$, subsequently. Therefore, by analyzing the system for sinusoidal voltage sources at the fundamental frequency, the results can be extended for square-wave voltages which is the output of the full bridges in MAB power conversion systems and will be considered in this research.

To realize the proposed multi-frequency system and to create independent frequency channels between each two voltage sources of the system, first, it must be found that over what time period the average transferred power between two phase shifted sinusoidal voltages with different frequencies is zero. Also, it must be determined that what should be the frequency of the sinusoidal voltages to have a zero average transferred power

between them. To address these questions for a system including two sinusoidal voltages connected through an inductor, like the one shown in Fig. 3, first the instantaneous power transferred from source 1 to source 2 must be found when the frequencies of the sources are different. If $v_1(t)$ is the voltage of the source 1 with the frequency, amplitude and phase of ω_1, V_1, φ_1 and $v_2(t)$ is the voltage of the source 2 with the frequency, amplitude and phase of ω_2, V_2, φ_2 , the instantaneous transferred power from source 1 to source 2 can be found by (18).

$$p_{12}(t) = v_1(t)(i_1(t) - i_2(t)) \quad (18)$$

Where

$$\begin{cases} v_1(t) = V_1 \sin(\omega_1 t + \varphi_1) \\ v_2(t) = V_2 \sin(\omega_2 t + \varphi_2) \end{cases} \quad (19)$$

And the currents $i_1(t)$ and $i_2(t)$ due to the voltages in sources 1 and 2 are

$$\begin{cases} i_1(t) = \frac{V_1}{\omega_1 L} \cos(\omega_1 t + \varphi_1) \\ i_2(t) = \frac{V_2}{\omega_2 L} \cos(\omega_2 t + \varphi_2) \end{cases} \quad (20)$$

And L is the linking inductance between the voltage sources.

By substituting (19) and (20) into (18), the instantaneous power is found as (21).

$$\begin{aligned} p_{12}(t) = & \frac{V_1^2}{2\omega_1 L} \sin(2\omega_1 t + 2\varphi_1) - \frac{V_1 V_2}{2\omega_2 L} (\sin((\omega_1 + \omega_2)t + \varphi_1 + \varphi_2) \\ & + \sin((\omega_1 - \omega_2)t + \varphi_1 - \varphi_2)) \end{aligned} \quad (21)$$

To find the time period over which the average transferred power is zero between two sinusoidal voltages with different frequencies, first, the analysis should be performed for the phase shift of zero in both voltage sources and then the effect of the phase shift can be considered later. Therefore, with $\varphi_1 = 0$ and $\varphi_2 = 0$, to have a zero average in (21), the integral of each individual term $\sin 2\omega_1 t$, $\sin((\omega_1 + \omega_2)t)$ and $\sin((\omega_1 - \omega_2)t)$ must be zero. Now, the question is that over what period of time the integral of all the three terms is zero. In the common divisors of $2\omega_1$, $(\omega_1 + \omega_2)$ and $(\omega_1 - \omega_2)$ the sinusoidal terms of $\sin 2\omega_1 t$, $\sin((\omega_1 + \omega_2)t)$ and $\sin((\omega_1 - \omega_2)t)$ are synchronized and, therefore, the average value of all of them is zero over every time period associated with the common divisors. If the frequency of ω_1 is considered as the reference frequency for the system, which must be selected according to the design requirements, the synchronization of the sinusoidal terms in equation (21) can occur in a time period associated with a common divisor less or greater than ω_1 . The synchronization happens in a value smaller than ω_1 only if $2\omega_1$, $(\omega_1 + \omega_2)$ and $|\omega_1 - \omega_2|$ are not congruent which results to have the synchronization in a time period much longer than the period associated with ω_1 and it is not desirable. Because, in a system with multiple ports and multiple frequency channels, the average transferred power must be found over a same time period for all the ports and the frequencies in the system, that is the smallest time period in which all the waveforms are synchronized. Therefore, the zero averaged transferred power must happen in a time period associated with common divisors greater than ω_1 . In order to have a common divisor at least equal to ω_1 , $(\omega_1 + \omega_2)$ and $(\omega_1 - \omega_2)$ must be an integer coefficient of ω_1 , as it is shown in (22), since the other term of $2\omega_1$ is itself an integer coefficient of ω_1 .

$$\begin{cases} \omega_1 + \omega_2 = k_1 \omega_1 \\ \omega_1 - \omega_2 = k_2 \omega_1 \end{cases} \quad k_1 \text{ and } k_2 \text{ are integers and } k_1, k_2 \neq 0 \text{ and } 1 \quad (22)$$

Now, the next question is that considering the frequency of the voltage source 1, ω_1 , as the reference frequency, what should be the frequency of the voltage source 2, ω_2 , to have a zero averaged transferred power between the sources in a time period associated with the common divisors greater than ω_1 . According to (22), and since k_1 and k_2 are integers, ω_2 must be an integer coefficient of ω_1 , as it is shown in (23).

$$\omega_2 = k \omega_1 \quad k \text{ is an integer and } k \neq 0 \quad (23)$$

$$\text{if } \begin{cases} k = \text{an odd number then the Least Common Divisor} = 2\omega_1 \\ k = \text{an even number then the Least Common Divisor} = \omega_1 \end{cases}$$

In (23), the least common divisor is the first frequency that sees the synchronization. According to this equation, if ω_2 is an odd integer coefficient of ω_1 , then the least common divisor between $2\omega_1$, $(\omega_1 + \omega_2)$ and $(\omega_1 - \omega_2)$ is $2\omega_1$, and if ω_2 is an even integer coefficient of ω_1 , then the least common divisor is ω_1 . So, what should be the value of the coefficient k ? Should it be an even or odd coefficient of ω_1 ? The answer is that it depends on the type of the voltage waveforms in the system. In case of sinusoidal voltages, odd coefficients lead to have the synchronization in a shorter period of time. However, in case of square-waves, which will be considered in this research, selecting odd coefficients results to have a non-zero averaged transferred power between the harmonics of the square-wave voltages. Because, square waves are included odd harmonics, in addition to the fundamental frequency, and selecting odd values for k will prevent to have an absolute

zero averaged power between the voltages. As the conclusion, in order to have a zero averaged power transferred between two square wave voltages, and in a time period associated with the reference frequency, considering the frequency of the voltage source 1 as the reference frequency, the frequency of the voltage source 2 must be an even coefficient of the reference frequency. This concept can be proven using Fig. 13 as well.

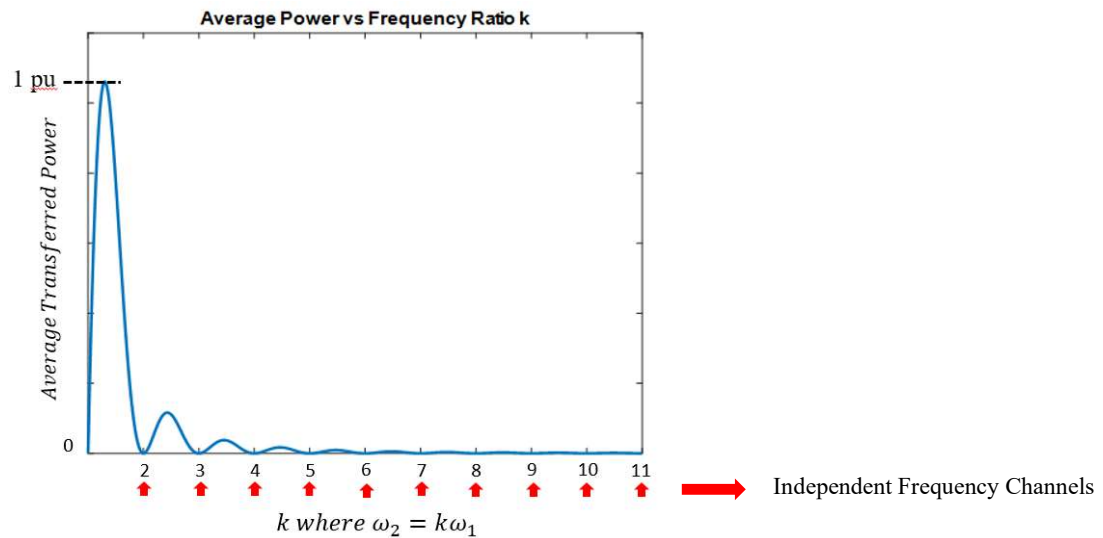


Figure 13 Average Power vs Frequency Ratio k Between Two Sinusoidal Voltages with Zero Phase Shifts

This figure shows the net power transferred between two sinusoidal voltages both with zero phase shift versus different frequency ratio k between the frequency of the source 1 and 2 (f_1 and f_2). As can be seen from the figure, although in high frequency ratios the average transferred power is approaching to zero in the non-integer coefficients of the reference frequency, the value of the average power is absolutely zero only at the integer coefficients of the reference frequency f_1 . Therefore, these frequencies can be considered

as the independent frequency channels to transfer power between the ports in a system with sinusoidal voltages.

As the summary of this discussion, in case of sinusoidal voltage sources, in order to have independent frequency channels to transfer power between two voltages with any amount of phase shift, the frequency of the channels must be an integer coefficient of the reference frequency. The only remaining question is that what about the square-wave voltage sources? In case of square-wave voltage sources, the frequency of the channels must be an even coefficient of the reference frequency to have independent frequency channels between the voltage sources in the system. In selecting the even coefficients of the reference frequency for the channels in a system with square wave voltage sources, it should be noted that for example the third harmonic of a channel with the fundamental frequency of $2f_1$, which is $6f_1$, can exchange power with the fundamental frequency of a channel with the frequency of $6f_1$. Therefore, a channel with the frequency of $6f_1$ cannot be considered as an independent frequency channel in a system with square-wave voltage sources. This is valid for any other frequencies which have an odd factor in their reference frequency coefficient like $10f_1$, $12f_1$, $14f_1$, etc.

Having investigated the concept of transferring power through independent frequency channels, now, it is the time to discuss multi-frequency multiport power conversion systems.

Concept of Multi-Frequency Power Conversion Systems

Fig. 14 shows a schematic of transferring power through multiple frequency channels in a multi-frequency multiport power system.

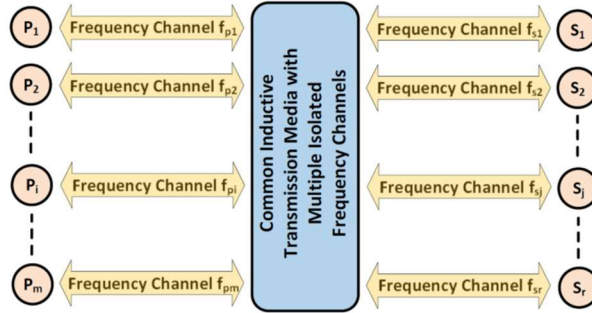


Figure 14 A Schematic of Multi-Frequency Multiport Power Systems

As can be seen from the figure, in this system, there are “m” ports in the primary side and “r” ports in the secondary side which interconnect through an inductive transmission media. A frequency channel is assigned to each port of the system through which power can be transferred bidirectionally between ports with the same frequencies independently from the others. Fig. 15 shows the circuit model of the system for square wave voltage sources.

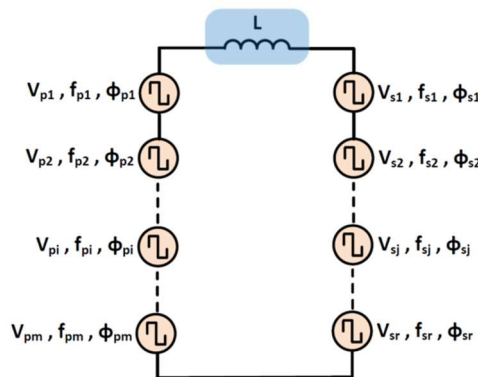


Figure 15 Circuit Model of Multi-Frequency Multiport Power Systems with Square-Wave Voltage Sources

In this figure, V_{pi} , f_{pi} and φ_{pi} denote the amplitude, frequency, and the phase of the source voltage “ i ” in the primary side of the system; V_{sj} , f_{sj} and φ_{sj} denote the amplitude, frequency and phase of the source voltage “ j ” in the secondary side of the system.

As it is mentioned previously, in order to have independent frequency channels, the frequency of each channel must be either equal to the reference frequency or an even coefficient of the reference frequency. Considering f as the reference frequency of the system, the frequencies f_{pi} and f_{sj} can be written as the coefficients k_{pi} and k_{sj} of the reference frequency, as it is shown in (24).

$$f_{pi} = k_{pi}f \quad (24)$$

$$f_{sj} = k_{sj}f$$

Where k_{pi} and k_{sj} can be 1, 2, 4, 8, ... according to the previous discussion for the frequency of the independent channels in a system with square wave voltages.

Now, to find the averaged transferred power between each two ports of the system through independent frequency channels, first the instantaneous power between each two ports with the same frequency must be found. Equation (25) shows the instantaneous power transferred from port i in the primary side to port j in the secondary side.

$$p_{pi_sj}(t) = v_{pi}(t)(i_{pi}(t) - i_{sj}(t)) \quad (25)$$

In addition to the power transferred between the ports in different sides, there are transferred powers between the series ports in the same side. Equation (26) shows the instantaneous power transferred from port i to port z both in the primary side.

$$p_{pi_pz}(t) = v_{pi}(t)(i_{pi}(t) + i_{pz}(t)) \quad (26)$$

In (25) and (26), $v_{pi}(t)$ is the instantaneous voltage of the port i in the primary side; $i_{pi}(t)$ is the current in the link when only $v_{pi}(t)$ is in the circuit; $i_{sj}(t)$ is the current in the link when only $v_{sj}(t)$ is in the circuit; $i_{pz}(t)$ is the current in the link when only $v_{pz}(t)$ is in the circuit. The voltage $v_{pi}(t)$ and the current of $i_{pi}(t)$ can be obtained by (27) and (28). The voltages of the other ports, and the currents due to the voltages can be found in similar functions.

$$v_{pi}(t) = \begin{cases} -V_{pi} & 0 < t < \frac{T\varphi_{pi}}{2\pi k_{pi}} \\ V_{pi} & \frac{T\varphi_{pi}}{2\pi k_{pi}} < t < \frac{T}{2k_{pi}} + \frac{T\varphi_{pi}}{2\pi k_{pi}} \\ -V_{pi} & \frac{T}{2k_{pi}} + \frac{T\varphi_{pi}}{2\pi k_{pi}} < t < \frac{T}{k_{pi}} + \frac{T\varphi_{pi}}{2\pi k_{pi}} \\ V_{pi} & \frac{T}{k_{pi}} + \frac{T\varphi_{pi}}{2\pi k_{pi}} < t < \frac{3T}{2k_{pi}} + \frac{T\varphi_{pi}}{2\pi k_{pi}} \\ -V_{pi} & \frac{3T}{2k_{pi}} + \frac{T\varphi_{pi}}{2\pi k_{pi}} < t < \frac{2T}{k_{pi}} + \frac{T\varphi_{pi}}{2\pi k_{pi}} \\ V_{pi} & \frac{2T}{k_{pi}} + \frac{T\varphi_{pi}}{2\pi k_{pi}} < t < \frac{5T}{2k_{pi}} + \frac{T\varphi_{pi}}{2\pi k_{pi}} \\ \vdots & \vdots \\ \vdots & \vdots \\ -V_{pi} & T - \frac{T}{2k_{pi}} + \frac{T\varphi_{pi}}{2\pi k_{pi}} < t < T \end{cases} \quad (27)$$

$$i_{pi}(t) = \begin{cases} i_L(0) - \frac{V_{pi}t}{L} & 0 < t < \frac{T\varphi_{pi}}{2\pi k_{pi}} \\ i_L(0) - \frac{V_{pi}(\frac{T\varphi_{pi}}{2\pi k_{pi}})}{L} + \frac{V_{pi}(t - \frac{T\varphi_{pi}}{2\pi k_{pi}})}{L} & \frac{T\varphi_{pi}}{2\pi k_{pi}} < t < \frac{T}{2k_{pi}} + \frac{T\varphi_{pi}}{2\pi k_{pi}} \\ i_L(0) - \frac{V_{pi}(\frac{T\varphi_{pi}}{2\pi k_{pi}})}{L} + \frac{V_{pi}(\frac{T}{2k_{pi}})}{L} - \frac{V_{pi}(t - \frac{T}{2k_{pi}} - \frac{T\varphi_{pi}}{2\pi k_{pi}})}{L} & \frac{T}{2k_{pi}} + \frac{T\varphi_{pi}}{2\pi k_{pi}} < t < \frac{T}{k_{pi}} + \frac{T\varphi_{pi}}{2\pi k_{pi}} \\ i_L(0) - \frac{V_{pi}(\frac{T\varphi_{pi}}{2\pi k_{pi}})}{L} + \frac{V_{pi}(t - \frac{T}{k_{pi}} - \frac{T\varphi_{pi}}{2\pi k_{pi}})}{L} & \frac{T}{k_{pi}} + \frac{T\varphi_{pi}}{2\pi k_{pi}} < t < \frac{3T}{2k_{pi}} + \frac{T\varphi_{pi}}{2\pi k_{pi}} \\ i_L(0) - \frac{V_{pi}(\frac{T\varphi_{pi}}{2\pi k_{pi}})}{L} + \frac{V_{pi}(\frac{T}{2k_{pi}})}{L} - \frac{V_{pi}(t - \frac{3T}{2k_{pi}} - \frac{T\varphi_{pi}}{2\pi k_{pi}})}{L} & \frac{3T}{2k_{pi}} + \frac{T\varphi_{pi}}{2\pi k_{pi}} < t < \frac{2T}{k_{pi}} + \frac{T\varphi_{pi}}{2\pi k_{pi}} \\ i_L(0) - \frac{V_{pi}(\frac{T\varphi_{pi}}{2\pi k_{pi}})}{L} + \frac{V_{pi}(t - \frac{2T}{k_{pi}} - \frac{T\varphi_{pi}}{2\pi k_{pi}})}{L} & \frac{2T}{k_{pi}} + \frac{T\varphi_{pi}}{2\pi k_{pi}} < t < \frac{5T}{2k_{pi}} + \frac{T\varphi_{pi}}{2\pi k_{pi}} \\ \vdots & \vdots \\ \vdots & \vdots \\ i_L(0) - \frac{V_{pi}(\frac{T\varphi_{pi}}{2\pi k_{pi}})}{L} + \frac{V_{pi}(\frac{T}{2k_{pi}})}{L} - \frac{V_{pi}(t - T + \frac{T}{2k_{pi}} - \frac{T\varphi_{pi}}{2\pi k_{pi}})}{L} & T - \frac{T}{2k_{pi}} + \frac{T\varphi_{pi}}{2\pi k_{pi}} < t < T \end{cases} \quad (28)$$

Where T is the time period associated with the reference frequency of f . As can be seen from (27) and (28), $v_{pi}(t)$ and $i_{pi}(t)$ are piecewise functions in which the number of pieces depends on the value of k_{pi} . The higher the value of k_{pi} the higher the number of the pieces.

Now, by finding the voltages and currents functions, the instantaneous power between each two ports of the system can be obtained using (25) and (26). The total instantaneous power in port i of the primary side of the system $p_{pi}(t)$ can be obtained by (29).

$$p_{pi}(t) = v_{pi}(t) \left(\sum_{i=1}^m i_{pi}(t) - \sum_{j=1}^r i_{sj}(t) \right) \quad (29)$$

And the total instantaneous power transferred from the primary side to the secondary side of the system $p_{p_s}(t)$ can be obtained by (30).

$$p_{p_s}(t) = \left(\sum_{i=1}^m v_{pi}(t) \right) \left(\sum_{i=1}^m i_{pi}(t) - \sum_{j=1}^r i_{sj}(t) \right) \quad (30)$$

Equations (29)-(30) are obtained based on the superposition theorem. According to (29), the average power in each port is obtained by the multiplication of the voltage in the port to the total current in the link. According to (30), the total instantaneous power transferred from the primary to the secondary side is obtained using the multiplication of the total voltage in the primary side to the total current in the link. Since the total voltage and the total current is calculated first and then they are multiplied, the superposition theorem is valid in these equations.

The averaged transferred power, then, can be obtained by making an integral of the instantaneous power over the time period of T which is the period associated with the reference frequency of f , as it is shown in (31).

$$P = \frac{1}{T} \int^T p(t) dt \quad (31)$$

According to (31), the averaged transferred power between port i in the primary side to port j in the secondary side both with the frequency of f_{pi} is obtained as (32).

$$P_{pi_sj} = \frac{V_{pi}V_{sj}}{(k_{pi})(2\pi fL)} (\varphi_{pi} - \varphi_{sj}) \left(1 - \frac{|\varphi_{pi} - \varphi_{sj}|}{\pi} \right) \quad \text{if} \quad f_{pi} = f_{sj} \quad (32)$$

And the averaged power transferred from port i to port z both in the primary side of the system and both with the frequency of f_{pi} is obtained as (33).

$$P_{pi_pz} = -\frac{V_{pi}V_{pz}}{(k_{pi})(2\pi fL)} (\varphi_{pi} - \varphi_{pz}) \left(1 - \frac{|\varphi_{pi} - \varphi_{pz}|}{\pi} \right) \quad \text{if} \quad f_{pi} = f_{pz} \quad (33)$$

Using (32) and (33), the total average power in each port, for example port i in the primary side, can be obtained by the summation of the transferred power between port i in the primary side and all the other ports with the same frequency, as it is shown in (34).

$$P_{pi} = \sum_{j=1}^r P_{pi_sj} + \sum_{z=1}^m P_{pi_pz} \quad \text{if} \quad f_{pi} = f_{pz} = f_{sj} \quad (34)$$

Also, the total average power in each side, for example in the primary side, can be obtained by the summation of the averaged power of all ports in that side. Equation (35) shows the total averaged power in the primary and the secondary side P_{p-s} and P_{s-p} .

$$P_{p-s} = \sum_{i=1}^m P_{pi} \quad \text{and} \quad P_{s-p} = \sum_{j=1}^r P_{sj} \quad \text{and} \quad P_{p-s} = -P_{s-p} \quad (35)$$

To better analyzing the system, a multi-frequency four-port power system with two ports in the primary side and two ports in the secondary side, as it is shown in Fig. 16, will be investigated in detail. This analysis can be extended to any number of ports in the primary or the secondary side as well.

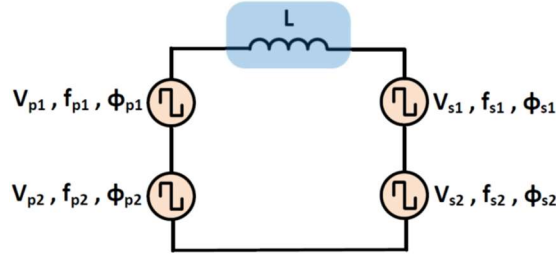


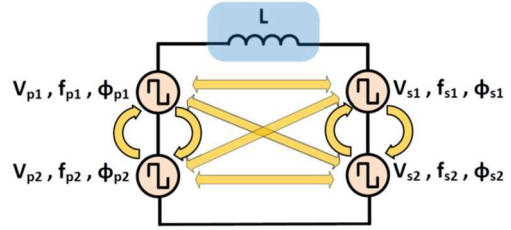
Figure 16 Circuit Model of Multi-Frequency Four-Port Power System with Two Ports in the Primary Side and Two Ports in the Secondary Side

The coefficients of the reference frequency in the system of Fig. 16 are k_{p1} , k_{p2} for the port 1 and port 2 in the primary side and k_{s1} , k_{s2} for the port 1 and port 2 in the secondary side. According to the different combinations of k_{p1} , k_{p2} , k_{s1} and k_{s2} , power can be transferred between any combination of the ports in the primary and the secondary side of the system. All the possibilities of transferring power between the ports in a multi-frequency four-port power system with two ports in the primary side and two ports in the

secondary side can be categorized in seven overall modes. Here are all the modes together with the averaged transferred power between the ports in each mode.

Mode 1:

$$k_{p1} = k_{p2} = k_{s1} = k_{s2}$$

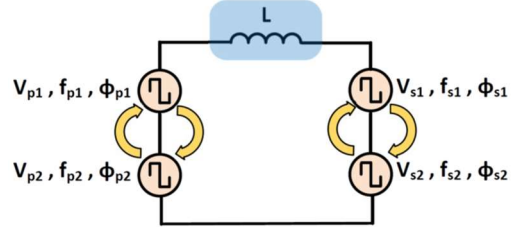


$$\begin{aligned} P_{p1} &= P_{p1_s1} + P_{p1_s2} + P_{p1_p2} & , & & P_{p2} &= P_{p2_s1} + P_{p2_s2} - P_{p1_p2} \\ P_{s1} &= -P_{p1_s1} - P_{p2_s1} + P_{s1_s2} & , & & P_{s2} &= -P_{p1_s2} - P_{p2_s2} - P_{s1_s2} \end{aligned}$$

$$\begin{aligned} P_{p-s} &= P_{p1} + P_{p2} = P_{p1_s1} + P_{p1_s2} + P_{p2_s1} + P_{p2_s2} \\ P_{s-p} &= P_{s1} + P_{s2} = -P_{p1_s1} - P_{p2_s1} - P_{p1_s2} - P_{p2_s2} \end{aligned}$$

Mode 2:

$$k_{p1} = k_{p2} \text{ and } k_{s1} = k_{s2} \text{ but } k_{p1} \neq k_{s1}$$

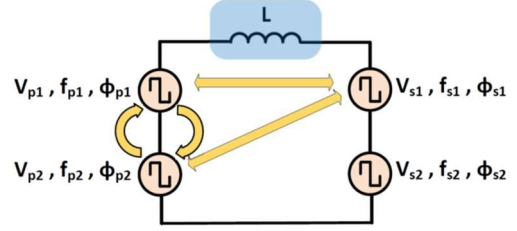


$$P_{p1} = P_{p1_p2} , \quad P_{p2} = -P_{p1_p2} , \quad P_{s1} = P_{s1_s2} , \quad P_{s2} = -P_{s1_s2}$$

$$P_{p-s} = P_{p1} + P_{p2} = 0 \quad , \quad P_{s-p} = P_{s1} + P_{s2} = 0$$

Mode 3:

- (a) $k_{p1} = k_{p2}$ and $k_{s1} \neq k_{s2}$
but $k_{p1} = k_{s1}$

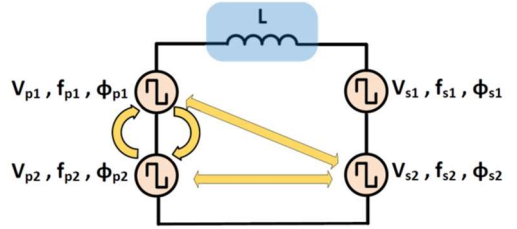


$$P_{p1} = P_{p1_s1} , P_{p2} = P_{p2_s1} , P_{s1} = -P_{p1_s1} - P_{p2_s1} , P_{s2} = 0$$

$$P_{p-s} = P_{p1} + P_{p2} = P_{p1_s1} + P_{p2_s1}$$

$$P_{s-p} = P_{s1} + P_{s2} = -P_{p1_s1} - P_{p2_s1}$$

- (b) $k_{p1} = k_{p2}$ and $k_{s1} \neq k_{s2}$
but $k_{p1} = k_{s2}$

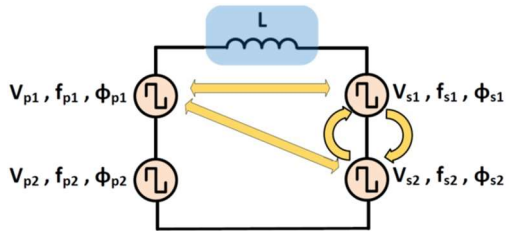


$$P_{p1} = P_{p1_s2} , P_{p2} = P_{p2_s2} , P_{s1} = 0 , P_{s2} = -P_{p1_s2} - P_{p2_s2}$$

$$P_{p-s} = P_{p1} + P_{p2} = P_{p1_s2} + P_{p2_s2}$$

$$P_{s-p} = P_{s1} + P_{s2} = -P_{p1_s2} - P_{p2_s2}$$

- (c) $k_{p1} \neq k_{p2}$ and $k_{s1} = k_{s2}$
but $k_{p1} = k_{s1}$

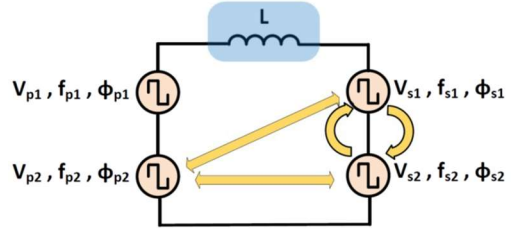


$$P_{p1} = P_{p1_s1} + P_{p1_s2} , P_{p2} = 0 , P_{s1} = -P_{p1_s1} , P_{s2} = -P_{p1_s2}$$

$$P_{p-s} = P_{p1} + P_{p2} = P_{p1_s1} + P_{p1_s2}$$

$$P_{s-p} = P_{s1} + P_{s2} = -P_{p1_s1} - P_{p1_s2}$$

- (d) $k_{p1} \neq k_{p2}$ and $k_{s1} = k_{s2}$
but $k_{p2} = k_{s1}$



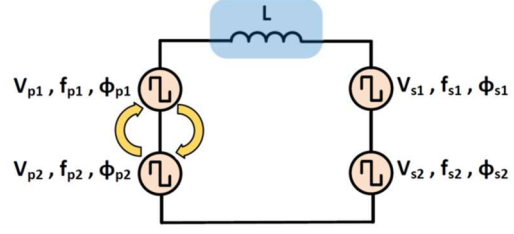
$$P_{p1} = 0, \quad P_{p2} = P_{p2_{s1}} + P_{p2_{s2}}, \quad P_{s1} = -P_{p2_{s1}}, \quad P_{s2} = -P_{p2_{s2}}$$

$$P_{p-s} = P_{p1} + P_{p2} = P_{p2_{s1}} + P_{p2_{s2}}$$

$$P_{s-p} = P_{s1} + P_{s2} = -P_{p2_{s1}} - P_{p2_{s2}}$$

Mode 4:

- (a) $k_{p1} = k_{p2}$ and $k_{s1} \neq k_{s2}$
but $k_{p1} \neq k_{s1}$ or $k_{p1} \neq k_{s2}$

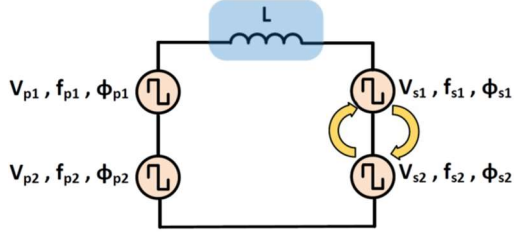


$$P_{p1} = P_{p1_{p2}}, \quad P_{p2} = -P_{p1_{p2}}, \quad P_{s1} = 0, \quad P_{s2} = 0$$

$$P_{p-s} = P_{p1} + P_{p2} = 0$$

$$P_{s-p} = P_{s1} + P_{s2} = 0$$

- (b) $k_{p1} \neq k_{p2}$ and $k_{s1} = k_{s2}$
but $k_{s1} \neq k_{p1}$ or $k_{s1} \neq k_{p2}$



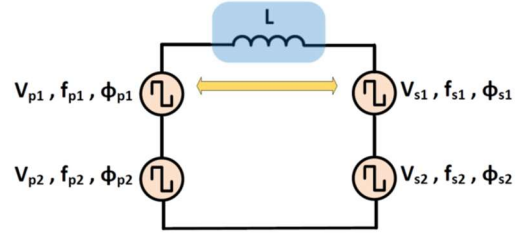
$$P_{p1} = 0, \quad P_{p2} = 0, \quad P_{s1} = P_{s1_{s2}}, \quad P_{s2} = -P_{s1_{s2}}$$

$$P_{p-s} = P_{p1} + P_{p2} = 0$$

$$P_{s-p} = P_{s1} + P_{s2} = 0$$

Mode 5:

- (a) $k_{p1} \neq k_{p2}$ and $k_{s1} \neq k_{s2}$
but $k_{p1} = k_{s1}$ and $k_{p2} \neq k_{s2}$

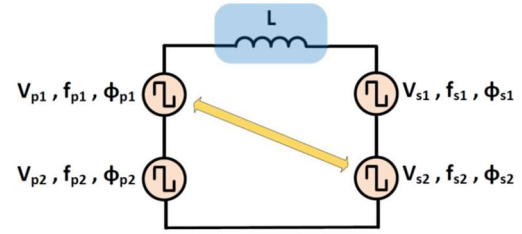


$$P_{p1} = P_{p1_s1}, \quad P_{p2} = 0, \quad P_{s1} = -P_{p1_s1}, \quad P_{s2} = 0$$

$$P_{p-s} = P_{p1} + P_{p2} = P_{p1_s1}$$

$$P_{s-p} = P_{s1} + P_{s2} = -P_{p1_s1}$$

- (b) $k_{p1} \neq k_{p2}$ and $k_{s1} \neq k_{s2}$
but $k_{p1} = k_{s2}$ and $k_{p2} \neq k_{s1}$

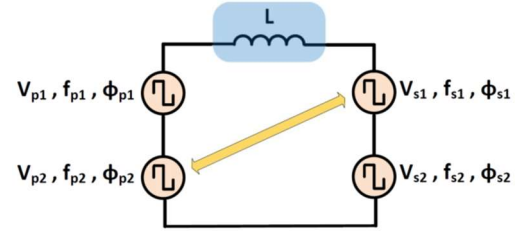


$$P_{p1} = P_{p1_s2}, \quad P_{p2} = 0, \quad P_{s1} = 0, \quad P_{s2} = -P_{p1_s2}$$

$$P_{p-s} = P_{p1} + P_{p2} = P_{p1_s2}$$

$$P_{s-p} = P_{s1} + P_{s2} = -P_{p1_s2}$$

- (c) $k_{p1} \neq k_{p2}$ and $k_{s1} \neq k_{s2}$
but $k_{p2} = k_{s1}$ and $k_{p1} \neq k_{s1}$

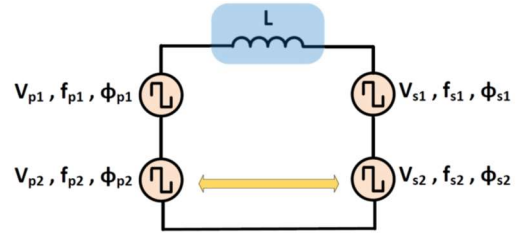


$$P_{p1} = 0, \quad P_{p2} = P_{p2_s1}, \quad P_{s1} = -P_{p2_s1}, \quad P_{s2} = 0$$

$$P_{p-s} = P_{p1} + P_{p2} = P_{p2_s1}$$

$$P_{s-p} = P_{s1} + P_{s2} = -P_{p2_s1}$$

- (d) $k_{p1} \neq k_{p2}$ and $k_{s1} \neq k_{s2}$
but $k_{p2} = k_{s2}$ and $k_{p2} \neq k_{s2}$



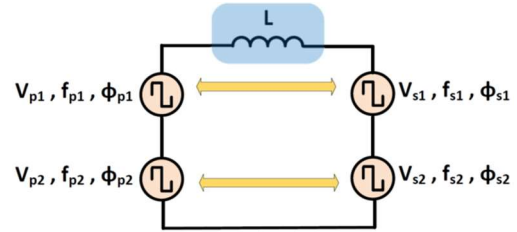
$$P_{p1} = 0, \quad P_{p2} = P_{p2_s2}, \quad P_{s1} = 0, \quad P_{s2} = -P_{p2_s2}$$

$$P_{p-s} = P_{p1} + P_{p2} = P_{p2_s2}$$

$$P_{s-p} = P_{s1} + P_{s2} = -P_{p2_s2}$$

Mode 6:

- (a) $k_{p1} \neq k_{p2}$ and $k_{s1} \neq k_{s2}$
but $k_{p1} = k_{s1}$ and $k_{p2} = k_{s2}$

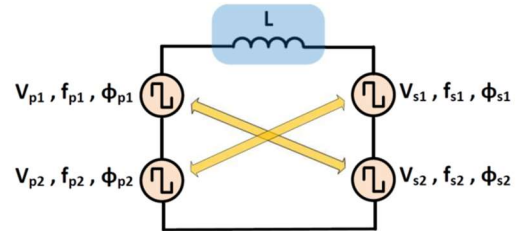


$$P_{p1} = P_{p1_s1}, \quad P_{p2} = P_{p2_s2}, \quad P_{s1} = -P_{p1_s1}, \quad P_{s2} = -P_{p2_s2}$$

$$P_{p-s} = P_{p1} + P_{p2} = P_{p1_s1} + P_{p2_s2}$$

$$P_{s-p} = P_{s1} + P_{s2} = -P_{p1_s1} - P_{p2_s2}$$

- (b) $k_{p1} \neq k_{p2}$ and $k_{s1} \neq k_{s2}$
but $k_{p1} = k_{s2}$ and $k_{p2} = k_{s1}$



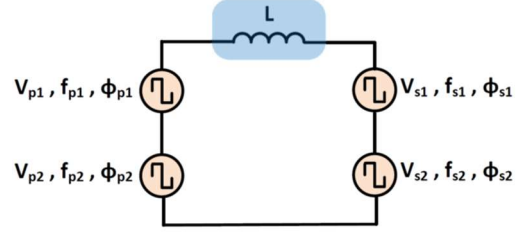
$$P_{p1} = P_{p1_s2}, \quad P_{p2} = P_{p2_s1}, \quad P_{s1} = -P_{p2_s1}, \quad P_{s2} = -P_{p1_s2}$$

$$P_{p-s} = P_{p1} + P_{p2} = P_{p1_s2} + P_{p2_s1}$$

$$P_{s-p} = P_{s1} + P_{s2} = -P_{p2_s1} - P_{p1_s2}$$

Mode 7:

$$k_{p1} \neq k_{p2} \neq k_{s1} \neq k_{s2}$$



$$P_{p1} = 0, P_{p2} = 0, P_{s1} = 0, P_{s2} = 0$$

$$P_{p-s} = P_{p1} + P_{p2} = 0$$

$$P_{s-p} = P_{s1} + P_{s2} = 0$$

Where $P_{p1-s1}, P_{p1-s2}, P_{p2-s1}, P_{p2-s2}, P_{p1-p2}$ and P_{s1-s2} can be found using (32)-(33).

In Mode 1, the frequency in all four ports is the same and, therefore, there is a transferred power between all ports of the system. In Mode 2, the frequency of the ports which are placed in the same side is the same and, as the result, there is no power transferred between the primary and the secondary side of the system. In Mode 3, the frequency of both ports in one side is equal and it is equal to the frequency of one of the ports in the other side as well. As the result, power is transferred from both ports in one side to one of the ports in the other side. In Mode 4, although the frequency of the ports in the same sides (primary or secondary) is the same, it is not equal to the frequency of the other side. Therefore, there is no transferred power between the primary and the secondary side. In Mode 5, the frequency of the ports which are placed in the same side are different, but the frequency of one of the ports in the primary side is equal to the frequency of one of the ports in the secondary side. As the result, there is a transferred power between only one of the ports in the primary side and one of the ports in the secondary side. In Mode 6, the frequency of the ports which are placed in the same side are different, but each one of the ports in the

primary side has an equal frequency to one of the ports in the secondary side. Therefore, there is a one-by-one transferred power between the ports in the primary and the secondary side. In Mode 7, the frequency in all ports of the system is different and there is no transferred power between the primary and the secondary side of the system.

Having discussed and analyzed the multi-frequency multiport power systems, it is the time to realize and implement it by an actual system called Multi-Frequency Multi Active Bridge (MFMAB) power conversion system, in this research. It will be discussed in the next chapter.

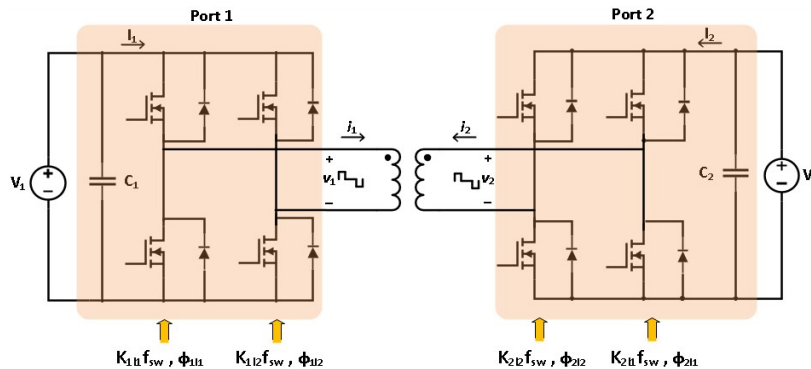
CHAPTER V

MULTI-FREQUENCY MULTI ACTIVE BRIDGE POWER CONVERSION SYSTEMS

A Multi-Frequency Multi Active Bridge power conversion system is a system including multiple full bridge converters which are linked magnetically through multiple inherently isolated frequency channels in the AC link. In order to realize the MFMAAB power conversion system, first, the concept of the power transfer through multiple frequencies channels must be analyzed in a Dual Active Bridge, and then it can be extended to higher number of ports.

Realization of Multi-Frequency Power Transfer in Dual Active Bridge Converter

The idea proposed in this research of power transfer through multiple frequencies in a Dual Active Bridge can be realized by assigning different frequencies to the legs of the converter, as it is shown in Fig. 17.



(a)

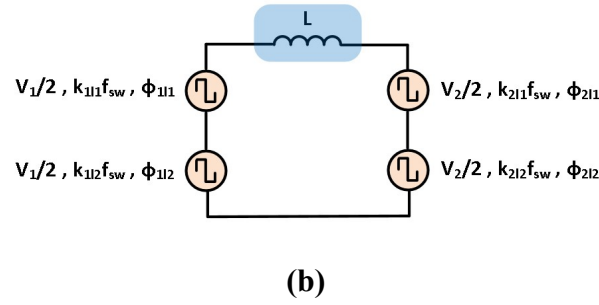


Figure 17 Multi-Frequency Multi-Phase Dual Active Bridge (a) Converter (b) Circuit Model

As can be seen from Fig. 17a, the legs of the converter are assigned with the frequencies of $k_{111}f_{sw}$, $k_{112}f_{sw}$, $k_{211}f_{sw}$ and $k_{212}f_{sw}$ and the phases of φ_{111} , φ_{112} , φ_{211} and φ_{212} . $k_{111}f_{sw}$ and φ_{111} are the frequency and the phase of the first leg of port 1; $k_{112}f_{sw}$ and φ_{112} are the frequency and the phase of the second leg of port 1; $k_{211}f_{sw}$ and φ_{211} are the frequency and the phase of the first leg of port 2; $k_{212}f_{sw}$ and φ_{212} are the frequency and the phase of the second leg of port 2. According to the discussion in chapter IV, the coefficients of k_{111} , k_{112} , k_{211} and k_{212} must be either one or an even number with no odd factor. This converter can be modeled by the circuit in Fig. 17b. As can be seen from this figure, each leg of the converter can be modeled by a voltage source with an amplitude of half of the DC bus voltage of the port. That is because, in fact, each leg of the converter works as a half bridge sharing a common DC bus with the other leg in same the port. According to Fig. 17b, the circuit model of a DAB with multiple frequencies and multiple phases in the legs is similar to the circuit model of a multi-frequency four-port system with two ports in the primary and two ports in the secondary side which has been discussed in Chapter IV. The only difference is in the amplitude of the voltage sources which is half

in the multi-frequency multi-phase DAB. Therefore, all the analysis which has been performed for the multi-frequency four-port system with two ports in the primary and two ports in the secondary side will be valid for the DAB with multiple frequencies and multiple phases in the legs as well. So, according to the frequency of the legs, there are seven modes for transferring power between the ports in a multi-frequency multi-phase DAB converter. The expressions for the averaged transferred power from the primary to the secondary side of the converter can be summarize in different modes as below.

Mode 1

$$k_{1l1} = k_{1l2} = k_{2l1} = k_{2l2}$$

$$P_{12} = P_{1l1_2l1} + P_{1l1_2l2} + P_{1l2_2l1} + P_{1l2_2l2}$$

Mode 2

$$k_{1l1} = k_{1l2} \text{ and } k_{2l1} = k_{2l2} \text{ but } k_{1l1} \neq k_{2l1}$$

$$P_{12} = 0$$

Mode 3

(a) $k_{1l1} = k_{1l2} \text{ and } k_{2l1} \neq k_{2l2} \text{ but } k_{1l1} = k_{2l1}$

$$P_{12} = P_{1l1_2l1} + P_{1l2_2l1}$$

(b) $k_{1l1} = k_{1l2} \text{ and } k_{2l1} \neq k_{2l2} \text{ but } k_{1l1} = k_{2l2}$

$$P_{12} = P_{1l1_2l2} + P_{1l2_2l2}$$

(c) $k_{1l1} \neq k_{1l2} \text{ and } k_{2l1} = k_{2l2} \text{ but } k_{1l1} = k_{2l1}$

$$P_{12} = P_{1l1_2l1} + P_{1l1_2l2}$$

(d) $k_{1l1} \neq k_{1l2} \text{ and } k_{2l1} = k_{2l2} \text{ but } k_{1l2} = k_{2l1}$

$$P_{12} = P_{1l2_2l1} + P_{1l2_2l2}$$

Mode 4:

$$(a) \quad k_{1l1} = k_{1l2} \text{ and } k_{2l1} \neq k_{2l2} \text{ but } k_{1l1} \neq k_{2l1} \text{ or } k_{1l1} \neq k_{2l2} \\ P_{12} = 0$$

$$(b) \quad k_{1l1} \neq k_{1l2} \text{ and } k_{2l1} = k_{2l2} \text{ but } k_{2l1} \neq k_{1l1} \text{ or } k_{2l1} \neq k_{1l2} \\ P_{12} = 0$$

Mode 5:

$$(a) \quad k_{1l1} \neq k_{1l2} \text{ and } k_{2l1} \neq k_{2l2} \text{ but } k_{1l1} = k_{2l1} \text{ and } k_{1l2} \neq k_{2l2} \\ P_{12} = P_{1l1_2l1}$$

$$(b) \quad k_{1l1} \neq k_{1l2} \text{ and } k_{2l1} \neq k_{2l2} \text{ but } k_{1l1} = k_{2l2} \text{ and } k_{1l2} \neq k_{2l1} \\ P_{12} = P_{1l1_2l2}$$

$$(c) \quad k_{1l1} \neq k_{1l2} \text{ and } k_{2l1} \neq k_{2l2} \text{ but } k_{1l2} = k_{2l1} \text{ and } k_{1l1} \neq k_{2l1} \\ P_{12} = P_{1l2_2l1}$$

$$(d) \quad k_{1l1} \neq k_{1l2} \text{ and } k_{2l1} \neq k_{2l2} \text{ but } k_{1l2} = k_{2l2} \text{ and } k_{1l2} \neq k_{2l1} \\ P_{12} = P_{1l2_2l2}$$

Mode 6:

$$(a) \quad k_{1l1} \neq k_{1l2} \text{ and } k_{2l1} \neq k_{2l2} \text{ but } k_{1l1} = k_{2l1} \text{ and } k_{1l2} = k_{2l2} \\ P_{12} = P_{1l1_2l1} + P_{1l2_2l2}$$

$$(b) \quad k_{1l1} \neq k_{1l2} \text{ and } k_{2l1} \neq k_{2l2} \text{ but } k_{1l1} = k_{2l2} \text{ and } k_{1l2} = k_{2l1} \\ P_{12} = P_{1l1_2l2} + P_{1l2_2l1}$$

Mode 7:

$$k_{1l1} \neq k_{1l2} \neq k_{2l1} \neq k_{2l2} \\ P_{12} = 0$$

Where P_{1l1_2l1} , P_{1l1_2l2} , P_{1l2_2l1} , and P_{1l2_2l2} can be found by (36).

$$\begin{aligned}
 P_{1l1_2l1} &= \frac{V_1 V_2}{8k_{1l1}\pi f_{sw} L} (\varphi_{1l1} - \varphi_{2l1}) \left(1 - \frac{|\varphi_{1l1} - \varphi_{2l1}|}{\pi} \right) \\
 P_{1l1_2l2} &= \frac{V_1 V_2}{8k_{1l1}\pi f_{sw} L} (\varphi_{1l1} - \varphi_{2l2}) \left(1 - \frac{|\varphi_{1l1} - \varphi_{2l2}|}{\pi} \right) \\
 P_{1l2_2l1} &= \frac{V_1 V_2}{8k_{1l2}\pi f_{sw} L} (\varphi_{1l2} - \varphi_{2l1}) \left(1 - \frac{|\varphi_{1l2} - \varphi_{2l1}|}{\pi} \right) \\
 P_{1l2_2l2} &= \frac{V_1 V_2}{8k_{1l2}\pi f_{sw} L} (\varphi_{1l2} - \varphi_{2l2}) \left(1 - \frac{|\varphi_{1l2} - \varphi_{2l2}|}{\pi} \right)
 \end{aligned} \tag{36}$$

In Mode 1, the frequency in all the legs is the same and the converter works as a conventional DAB but with multiple phases. In Mode 2, the frequency of the legs in a same port is equal, but the frequencies of the ports are different. In Mode 3, the frequency of the legs in one port is the same and it is equal to the frequency of one of the legs in the other port. In Mode 4, the frequency of the legs in one of the ports is the same but it is different with the frequency of legs in the other port. In Mode 5, the frequencies of the legs which are placed in a same port are different, but the frequency of one of the legs in port 1 is equal to the frequency of one of the legs in port 2. In Mode 6, the frequencies of the legs which are placed in a same port are different, but the frequency of each one of the legs in port 1 is equal to one of the legs in port 2. In Mode 7, the frequencies in all the legs are different.

Having discussed the concept of power transfer in a DAB with multiple frequencies and phases in legs, this concept can be extended to the systems with higher number of ports called Multi-Frequency Multi-Phase Multiple Active Bridge (MFMP MAB) power conversion system, in this research.

Multi-Frequency Multi-Phase Multi Active Bridge Power Conversion System

Fig. 18 shows a N-port MFMP MAB power conversion system.

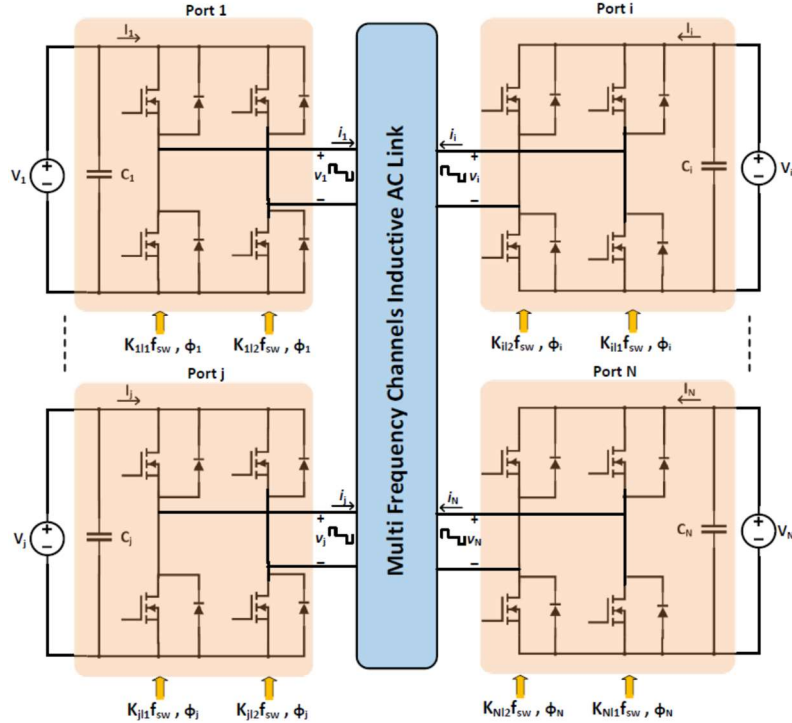
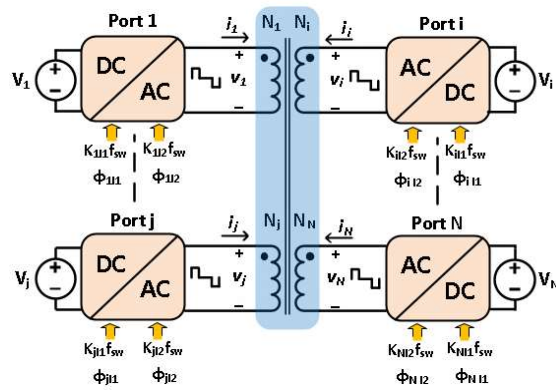
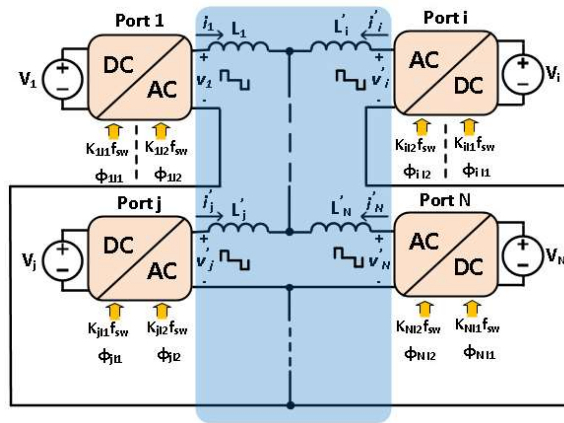


Figure 18 Multi-Frequency Multi-Phase Multi Active Bridge Power Conversion System

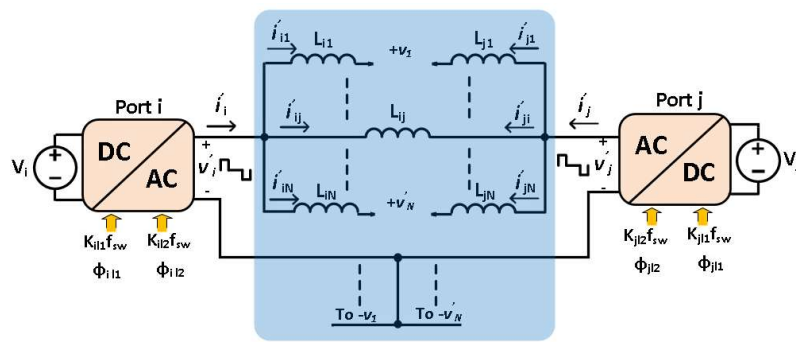
As can be seen from Fig. 18, each port “ i ” is assigned with two frequencies $k_{i1} f_{sw}, k_{i2} f_{sw}$ and two phases ϕ_{i1}, ϕ_{i2} which are the frequency and phase of the first leg and the second leg of port “ i ” of the system, subsequently. The multi-frequency channel inductive AC link can be a N-winding transformer, or N individual parallel connected transformers. In this research, the N-winding transformer will be considered as the multi-frequency channel inductive AC link in the system because of having one core instead of N separate cores in comparison to parallel connected transformers and higher power management capability. Fig. 19 shows a schematic MFMP MAB power conversion system with a multi-winding transformer in the AC link together with its circuit models.



(a)



(b)



(c)

Figure 19 MFMP MAB Power Conversion System Multi-Winding Transformer in the AC link: (a) Schematic (b) Star Circuit Model (c) Delta Circuit Model

Current, voltage, and inductance of each port “ i ” can be found by (7), and the linking inductance between each two ports “ i ” and “ j ”, L_{ij} , in the delta circuit model can be found by (9). Using the delta circuit model, the expression for the transferred power between each two ports of a MFMF MAB power conversion system can be found using (37).

$$P_{ij} = P_{il1} + P_{il2} \quad (37)$$

$$P_{ji} = P_{jl1} + P_{jl2} = -P_{ji}$$

Where

$$P_{il1} = -P_{il1_{il2}} + P_{il1_{jl1}} + P_{il1_{jl2}} \quad (38)$$

$$P_{il2} = P_{il1_{il2}} + P_{il2_{jl1}} + P_{il_{jl}}$$

$$P_{jl1} = -P_{il_{jl1}} - P_{il2_{jl1}} - P_{jl1_{jl}}$$

$$P_{jl2} = -P_{il1_{jl2}} - P_{il2_{jl2}} + P_{jl1_{jl2}}$$

And

$$\text{if } k_{il1} = k_{il2}: P_{il1_{il2}} = \frac{V_i^2}{8k_{il1}\pi f_{sw}L_{ij}} (\varphi_{il1} - \varphi_{il2}) \left(1 - \frac{|\varphi_{il1} - \varphi_{il2}|}{\pi} \right) \quad (39)$$

$$\text{if } k_{il} = k_{jl1}: P_{il1_{jl1}} = \frac{V_i V_j}{8k_{il1}\pi f_{sw}L_{ij}} (\varphi_{il1} - \varphi_{jl1}) \left(1 - \frac{|\varphi_{il1} - \varphi_{jl1}|}{\pi} \right)$$

$$\text{if } k_{il1} = k_{jl2}: P_{il1_{jl2}} = \frac{V_i V_j}{8k_{il1}\pi f_{sw}L_{ij}} (\varphi_{il} - \varphi_{jl}) \left(1 - \frac{|\varphi_{il} - \varphi_{jl}|}{\pi} \right)$$

$$\text{if } k_{il2} = k_{jl} : P_{il2_{jl}} = \frac{V_i V_j}{8k_{il2}\pi f_{sw}L_{ij}} (\varphi_{il} - \varphi_{jl1}) \left(1 - \frac{|\varphi_{il2} - \varphi_{jl}|}{\pi} \right)$$

$$\text{if } k_{il} = k_{jl} : P_{il_{jl1}} = \frac{V_i V_j}{8k_{il2}\pi f_{sw}L_{ij}} (\varphi_{il} - \varphi_{jl}) \left(1 - \frac{|\varphi_{il} - \varphi_{jl}|}{\pi} \right)$$

$$\text{if } k_{j11} = k_{j12}: P_{j11_j12} = \frac{V_j^2}{8k_{jl} \pi f_{sw} L_{ij}} (\varphi_{j11} - \varphi_{j12}) \left(1 - \frac{|\varphi_{j11} - \varphi_{j12}|}{\pi}\right)$$

Otherwise, they are zero.

Also, the total power in each port “*i*” can be found by (40).

$$P_i = \sum_{i \neq j}^N P_{ij} \quad (40)$$

In a N-port MFMP MAB power conversion system, to obtain the maximum power transfer capability through isolated frequency channels, there are $N-1$ options for the coefficient of the reference switching frequency in each leg of the converter, each one of which must be either one or an even number without an odd factor. Therefore, for a N-port system, there are totally $(N - 1)^{2N}$ modes of transferring power between the ports. According to the number of the ports and the frequency of the legs, there are five possibilities to create independent frequency channels in MFMP MAB power conversion systems:

- One independent frequency channel between each selected two ports “*i*” and “*j*”
- Two independent frequency channels between each selected port “*i*” and two other selected ports “*j*” and “*z*” at the same time
- One independent frequency channel between one leg of each selected port “*i*” and both legs of another selected port “*j*”
- One independent frequency channel between one leg of each selected port “*i*” and one leg of another selected port “*j*”
- Two independent frequency channels between each two selected ports “*i*” and “*j*”.

To better illustrate each one these conditions, a three-port version of the system called Multi-Frequency Multi-Phase Triple Active Bridge (MFMP TAB) will be discussed in detail.

Multi-Frequency Triple Active Bridge Power Conversion System

Fig. 20 shows a MFMP TAB power conversion system with a three-winding transformer in the AC link.

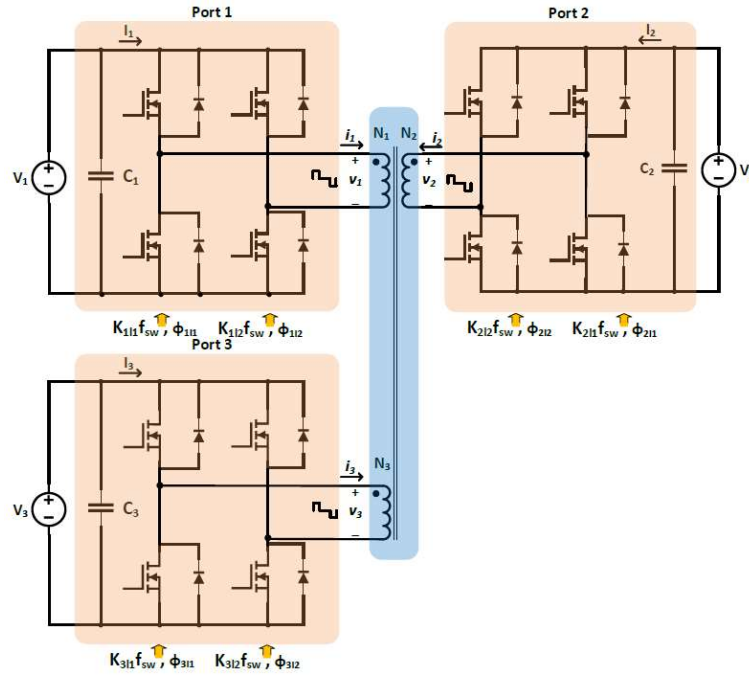


Figure 20 Multi-Frequency Multi-Phase Triple Active Bridge Power Conversion System with Three-Winding Transformer in AC Link

As it is shown in this figure, the frequency and phase of the legs are $k_{111}f_{sw}$, $k_{112}f_{sw}$, φ_{111} , φ_{112} in port 1; $k_{211}f_{sw}$, $k_{212}f_{sw}$, φ_{211} , φ_{212} in port 2, and $k_{311}f_{sw}$, $k_{312}f_{sw}$, φ_{311} , φ_{312} in port 3. As it was mentioned before, f_{sw} is the reference switching frequency that must be determined according to the design requirement. In order to take the maximum power transfer capability of the system with isolated frequency channels between the ports, it can be proven that the coefficients of k_{111} , k_{112} , k_{211} , k_{212} , k_{311} and k_{312} must be either 1 or 2 in a three-port system. All the possible modes of transferring power between the ports can

be covered using these two coefficients of the reference frequency. The power transfer capability is maximized using these two coefficients in a MFMP TAB since the lower the coefficient of the reference frequency the higher the power transfer capability of the converter. Therefore, having two options for each one of k_{111} , k_{112} , k_{211} , k_{212} , k_{311} and k_{312} , there are totally $2^6 = 64$ modes of transferring power between the ports in a MFMP TAB power conversion system. All the modes of transferring power between the ports in a MFMP TAB power conversion system can be categorized in five overall modes, as it is shown in Fig. 21. It can be proven that all the other modes can be subcategorized under one of these five modes in a three-port system.

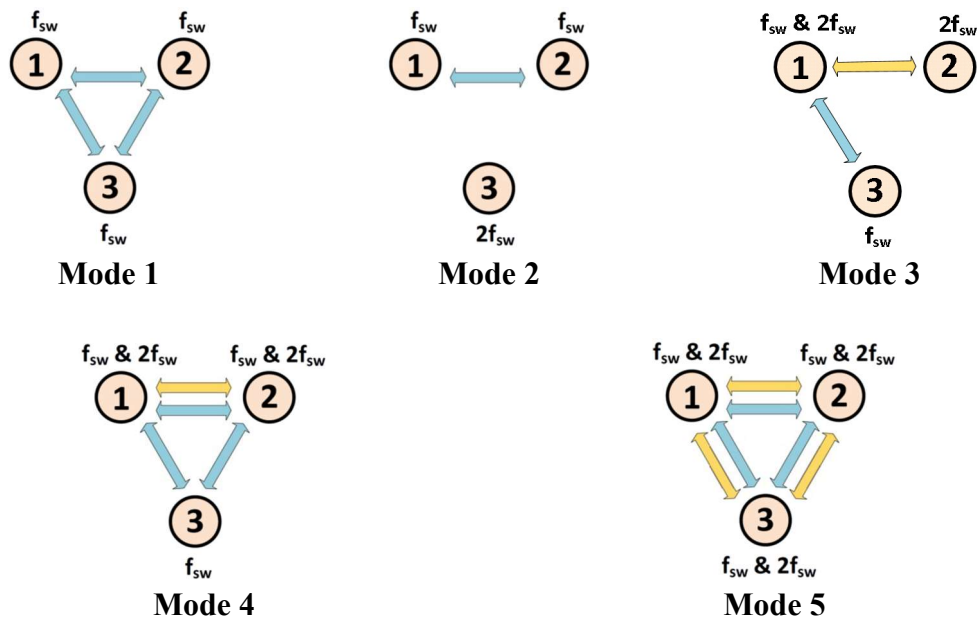


Figure 21 Transferring Power Modes in Multi Frequency Multi-Phase Triple Active Bridge Power Conversion System with Three-Winding Transformer in the AC Link

Mode 1 shows a power flow diagram in the conventional TAB in which power can be transferred bidirectionally based on the phase shift between the ports. However, the power transfer in each port is dependent to the others in this mode. To transfer power directly

from one port to one another without interchanging power with the third port, the switching frequency of the third port must be set on a different value which must be $2f_{sw}$ in a three-port system, as it is shown in Mode 2.

In Mode 3, by setting the frequency of one of the ports on f_{sw} & $2f_{sw}$, which can be realized by assigning f_{sw} in one of the legs and $2f_{sw}$ in the other one, the port with the frequency of f_{sw} & $2f_{sw}$ can transfer power, at the same time, to the ports with the frequency of f_{sw} and $2f_{sw}$ through two isolated frequency channels without interfering with each other. In this way, there will not be any power transferred between the ports with the frequency of f_{sw} and $2f_{sw}$, and the power in these ports can be controlled independently through frequency channels of f_{sw} and $2f_{sw}$. This mode of operation is useful in three-port systems with two sources and one load or one source and two loads, especially when there are unbalanced load demands, unequal source voltages, limitations in supplying power in the sources, failures in one or more ports, or unequal linking inductances. In a system with two sources and one load, if the voltages of the source ports are unequal, or if different supplying powers are required from sources, based on the system power management strategy, by operating in Mode 3, the power flow can be controlled between the load and each one of the sources independently without transferring power between the source ports. This can happen by setting the frequency of the load port on f_{sw} & $2f_{sw}$, frequency of one the sources on f_{sw} and the other one on $2f_{sw}$. In a system with one source and two loads with unbalanced power demands, by operating in Mode 3, the power flow between the source port and each one of the loads can be controlled independently without transferring power between the load ports. This can happen by setting the frequency of the

source port on f_{sw} & $2f_{sw}$, frequency of one the loads on f_{sw} and the other one on $2f_{sw}$. In Mode 4 and Mode 5, power can be transferred between two ports both with the frequency of f_{sw} & $2f_{sw}$ through two isolated frequency channels but through a common link. These modes of operations are useful when different quality of the power is required by the loads from one of the sources. By operating I Mode 4 and Mode 5, the high-quality power can be transferred through the frequency channel of $2f_{sw}$, and the low-quality power through the frequency channel of f_{sw} .

In order to analyze the independent power transfer capability of the proposed system, the averaged transferred power versus phase shift is depicted in Fig. (22) for the one source/two loads condition, and in Fig. (23)-(24) for the two sources/one load condition. The specification of the sampled system is selected according to the MEA power system which is shown in Table. 1.

To simplify analysis of the system, a same linking inductance is assumed for all ports:

$$L_{12} = L_{13} = L_{23} = L$$

Also, a common phase shift is considered for both legs of each port as below:

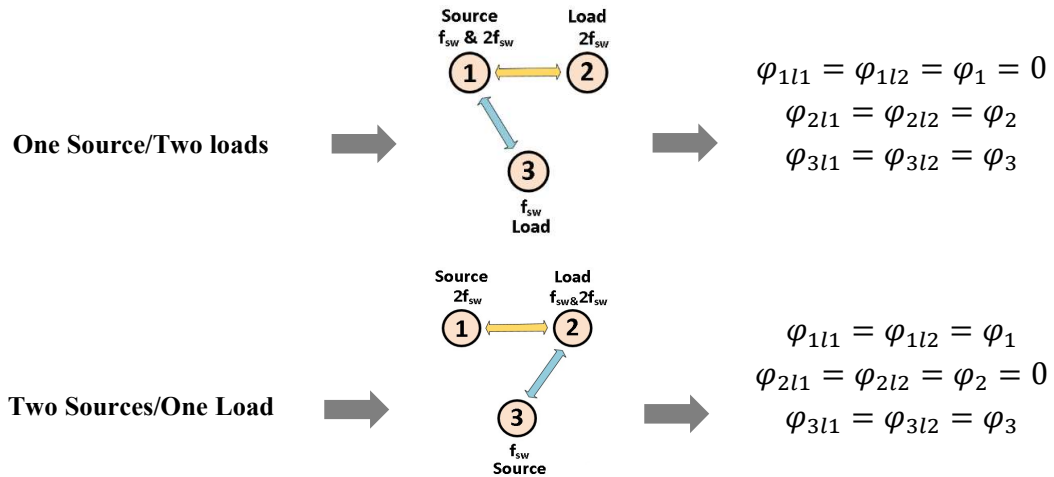
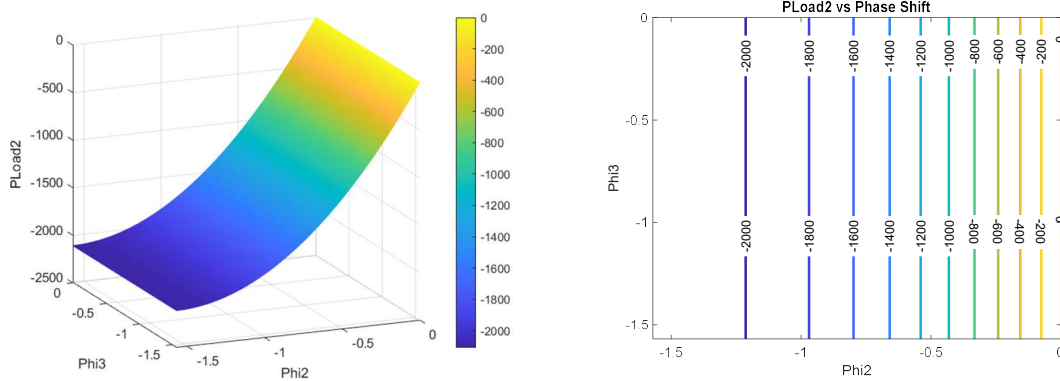
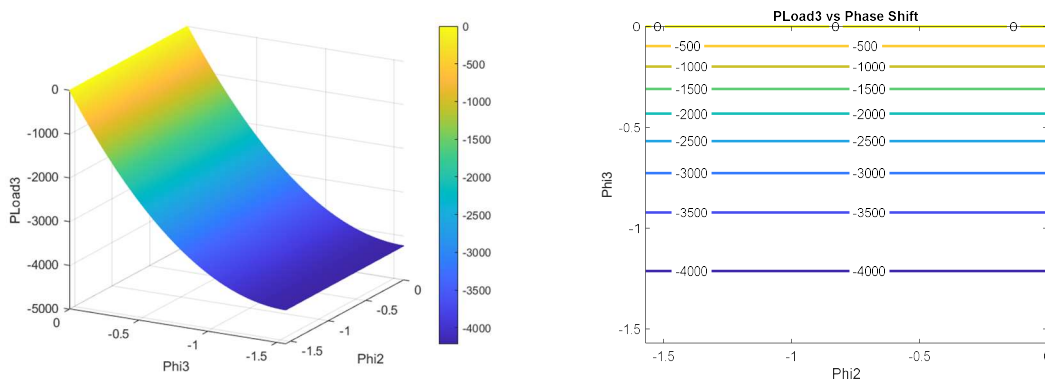


Table 1 More Electric Aircraft Power System Specification

Port 1 Voltage: V_1	270 V
Port 2 Voltage: V_2	27 V
Port 3 Voltage: V_3	135 V
Turn Ratio: $N_1: N_2: N_3$	10:1:5
Switching Frequency: f_{sw}	20 kHz
Linking Inductance: L	54 μ H

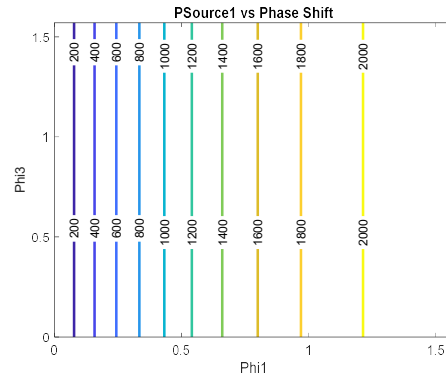
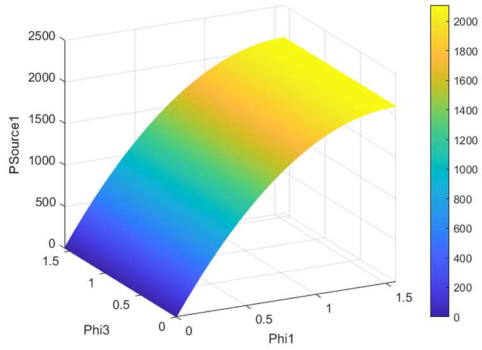


(a)

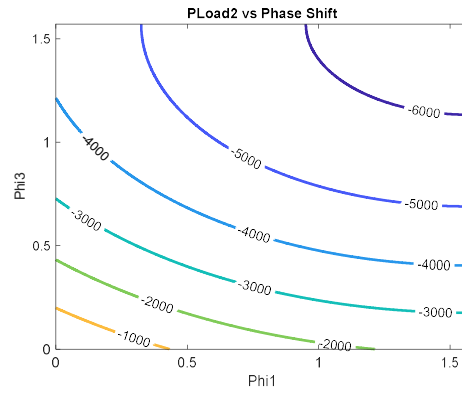
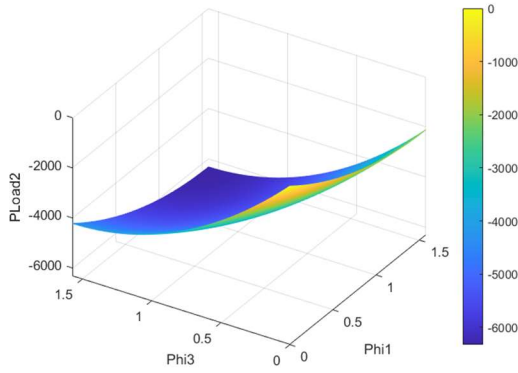


(b)

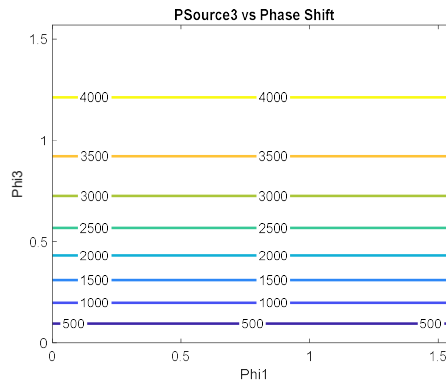
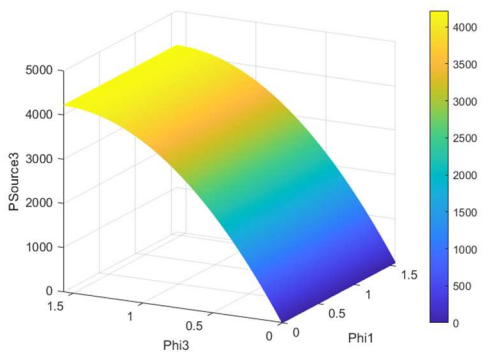
Figure 22 Load Power vs Phase Shift in a One Source/ Two Loads Multi-Frequency Triple Active Bridge Power Conversion System (a) Load Port 2 (b) Load Port 3



(a)



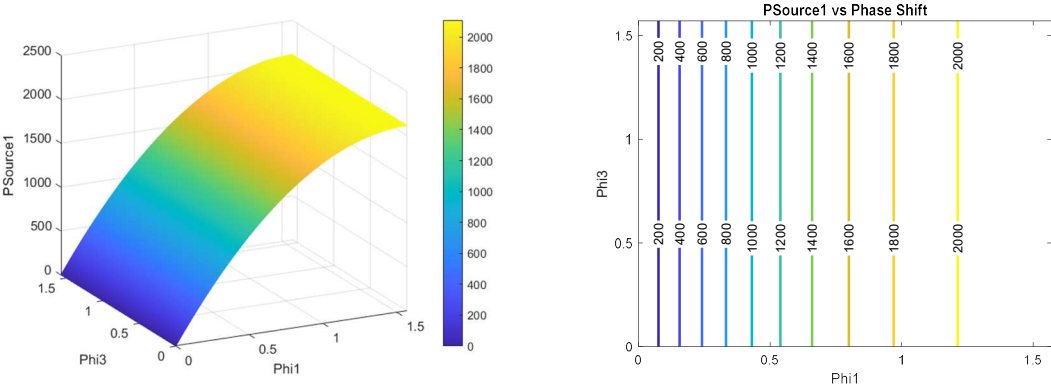
(b)



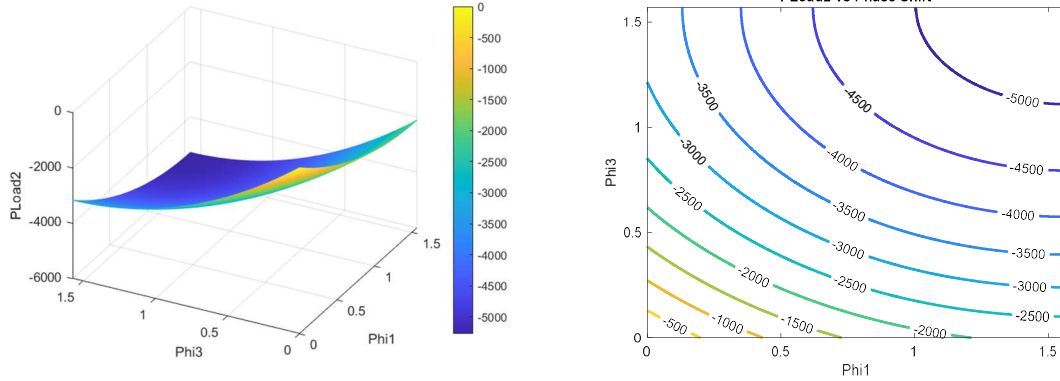
(c)

Figure 23 Averaged Transferred Power vs Phase Shift in a Two Sources/ One Load Multi-Frequency Triple Active Bridge Power Conversion System (a) Source Port 1 (b) Load Port 2 (c) Source Port 3

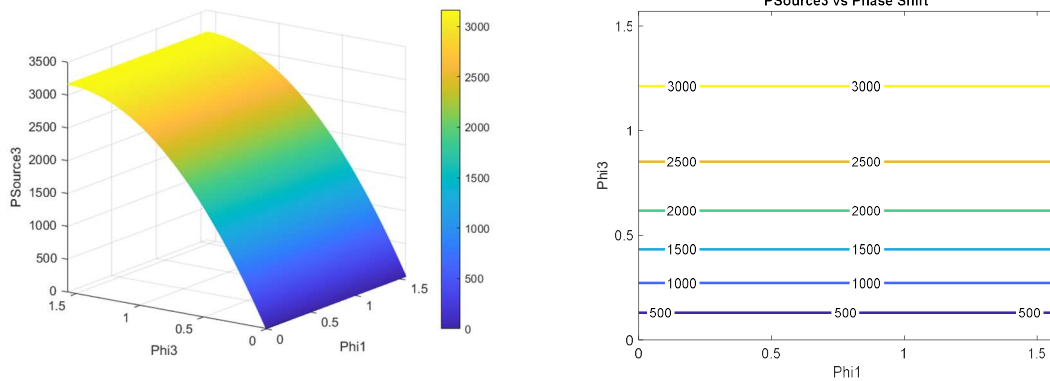
As can be seen in Fig. 22, the load power in port 2 changes only with changing φ_2 and there is no change in the transferred power to the load in port 2 with changing φ_3 . Also, the load power in port 3 is changed only with changing φ_3 and there is no change in the transferred power to the load in port 3 with changing φ_2 . This means an independent power flow in each load port which leads to have the full dynamic range for the phases φ_2 and φ_3 . This analysis is valid for the source ports in Fig. 23 as well. The value of the supplying power in the source port 1 and source port 3 can be controlled only with their own phase shifts, φ_1 and φ_3 respectively and changing the phase shift in the other port does not have any effect on the value of the supplying power from each port. Fig. 24 shows the averaged transferred power vs phase shift in a two Sources/ one load system with 25% drop in the source voltage in port 3.



(a)



(b)



(c)

Figure 24 Averaged Transferred Power vs Phase Shift in a Two Sources/ One Load Multi-Frequency Triple Active Bridge Power Conversion System with 25% Drop in the Source Voltage 3 (a) Source Port 1 (b) Load Port 2 (c) Source Port 3

As can be seen for this figure, by reducing the voltage in the source port 3, the amount of the power flow is changed only between the source port 3 and the load port 2, and there is no change in the transferred power in the source port 1. This shows an independent power flow between each source and the load port.

For the proof-of-concept validation, the MF TAB power conversion system will be implemented by both simulation and experiment in the next chapters.

CHAPTER VI

SIMULATION AND EXPERIMENTAL VALIDATION

Simulation of Multi-Frequency Triple Active Bridge Power Conversion System

Fig. 25 shows a schematic of a MFTAB power conversion system control diagram including a power management module and the voltage and current control loops which will be implemented in this research.

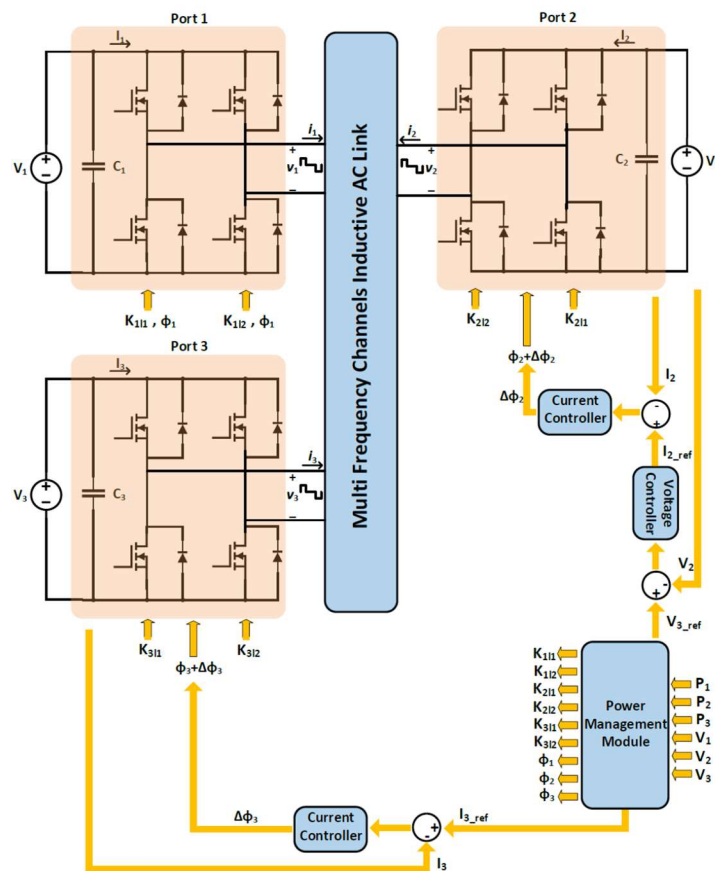


Figure 25 Multi-Frequency Triple Active Bridge Power Conversion System

As can be seen from the figure, there is power supply in port 1, a resistive load in port 2, and a battery in port 3. The power management module is responsible to generate the optimum phase shifts and the coefficients of the reference switching frequency according

to the source voltages and load demands. For the port connected to the battery, since the voltage of the port is regulated by the battery, only a current controller loop is required to regulate the current in the port according to the demanded power. For the port connected to the resistive load, both voltage and current controller is required to regulate the voltage of the port, and to meet the demanded power. This system has been simulated for one source/ two loads, two sources/ one load, and one source/ one load/ one port with zero power conditions. In the simulated system, the DC bus capacitors are $C_1 = C_2 = C_3 = 0.68 \text{ mF}$, the leakage inductances of the three-winding transformer are $L_1 = L_2 = L_3 = 18 \text{ } \mu\text{H}$, and the turn ratio of the transformer $N_1 : N_2 : N_3$ is 10: 1: 5.

The simulated system has been validated both in transient and static conditions. Table. 2 shows the operation condition of the one source/ two loads system in simulation.

Table 2 Operation Condition in Simulated One Source/ Two loads System

One Source / Two Loads			
Port No.	Port 1	Port 2	Port 3
Source/ Load	Source	Load	Load
Frequency	20 kHz & 40 kHz	40 kHz	20 kHz
DC Bus Voltage	270 V	27 V	135 V
Power	2 kW → 1500 W	1 kW → 500 W	1 kW
Phase	0.3577	1.5708 → 0.7893	0.7893

As can be seen from the table, the source port has the frequency of 20 kHz & 40 kHz, the load port 2 has the frequency of 40 kHz, and the load port 3 has the frequency of 20 kHz.

At the beginning of the simulation, the demanded power in the load port 2 and load port 3 are both 1 kW, and therefore the supplying power in the source port 1 is 2 kW. At the time of 0.15 seconds, there is a change to the demanded power in load port 2 from 1 kW to 500 W, which subsequently results in a reduction of 500W in the source port 1. The simulation results are shown in Fig. (26)-(28).

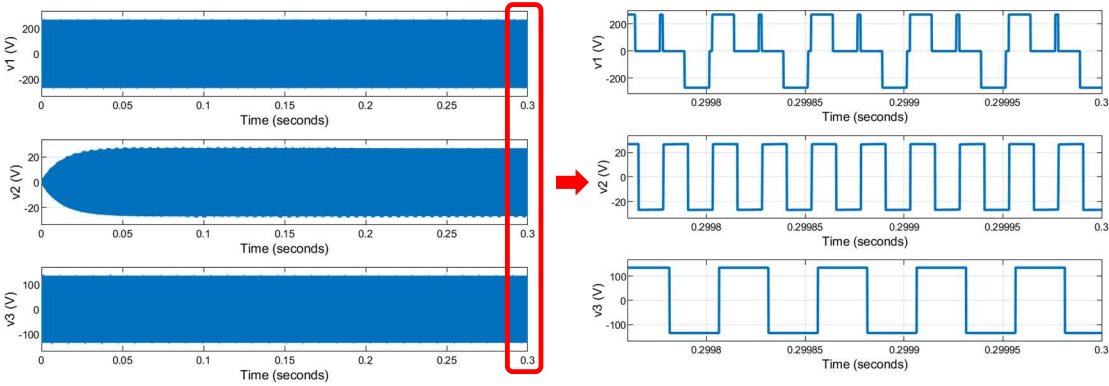


Figure 26 AC Voltages in One Source/ Two Loads

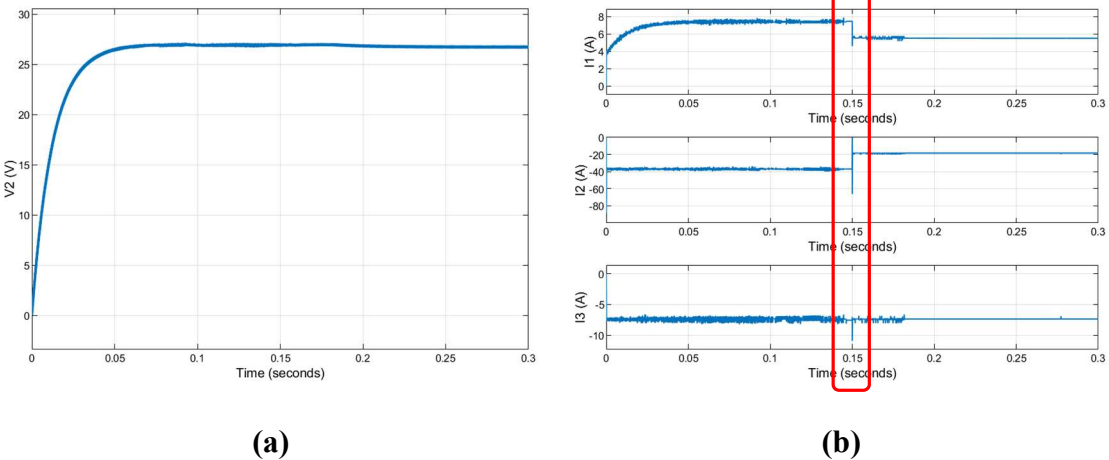
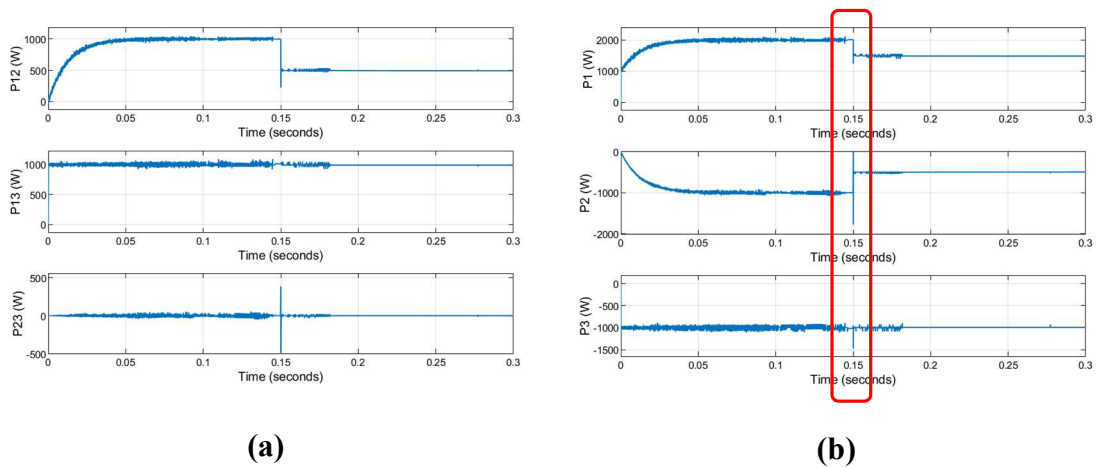


Figure 27 Load Port 2 DC Voltage, and DC Currents in One Source / Two Loads: (a) Resistive Load Port DC Voltage (b) DC Currents



**Figure 28 Linking Transferred Power and Port Power in One Source/ Two Loads:
 (a) Linking Transferred Power (b) Port Power**

Fig. 26 shows the AC voltages in the AC link of the system. As can be seen from this figure, the voltage in the resistive load port 2 ramps up in the transient state and reaches to the expected value of 27 V in the steady-state condition. Fig. 27 shows the DC bus voltage in the resistive load port 2, and the DC currents in all ports. As can be seen from from Fig. 27a, the DC voltage of the resistive load is established on 27 V after a smooth transient. According to Fig. 27b, by reducing the demanded power in the load port 2 in 0.15 S, the current in port 2 is reduced, and as the result of that, there is a reduction in the source port 1 current, proportionally. But, the point is that there is no change in the value of the current in the load port 3 after changing the current in the load port 1. This shows that changing the phase shift between the load port 3 and the source port 1 does not have any effect on the load power in port 2. In other words, the demanded power in the load ports can be controlled independently from each other. This is shown in Fig. 28 as well. As can be seen from Fig. 28a, by changing the demanded power in the load port 2, there is only a change in the transferred power from source port 1 to load port 2 and there is no

change in the value of the transferred power between the source port 1 and the load port 3. Also, the transferred power between the load ports, P_{23} , is zero. The performance of the system can be validated by Fig. 28b as well. As can be seen from this figure, all the ports follow the expected powers, accurately both before and after the reduction in the demanded load power in port 2, without any interference between the load ports.

Table. 3 shows the operation condition of the two sources/ one load system in simulation.

Table 3 Operation Condition in Simulated Two Sources/ One Load System

Two Sources / One Load			
Port No.	Port 1	Port 2	Port 3
Source/ Load	Source	Load	Source
Frequency	40 kHz	20 kHz & 40 kHz	20 kHz
DC Bus Voltage	270 V	27 V	135
Power	1 kW	2 kW → 1500 W	1 kW → 500 W
Phase	1.1057	1.5374	1.3386 → 1.4414

As can be seen from the table, the load port has the frequency of 20 kHz & 40 kHz, the source port 1 has the frequency of 40 kHz, and the source port 3 has the frequency of 20 kHz. At the beginning of the simulation, the supplying power in each one of the source ports is 1 kW, and therefore the load power in port 2 is 2 kW. At the time of 0.15 seconds, there is a change in the supplying power of the source port 3 from 1 kW to 500 W, which subsequently results in a reduction in the load port to 1500 W. The simulation results for this condition are shown in Fig. (29)-(31).

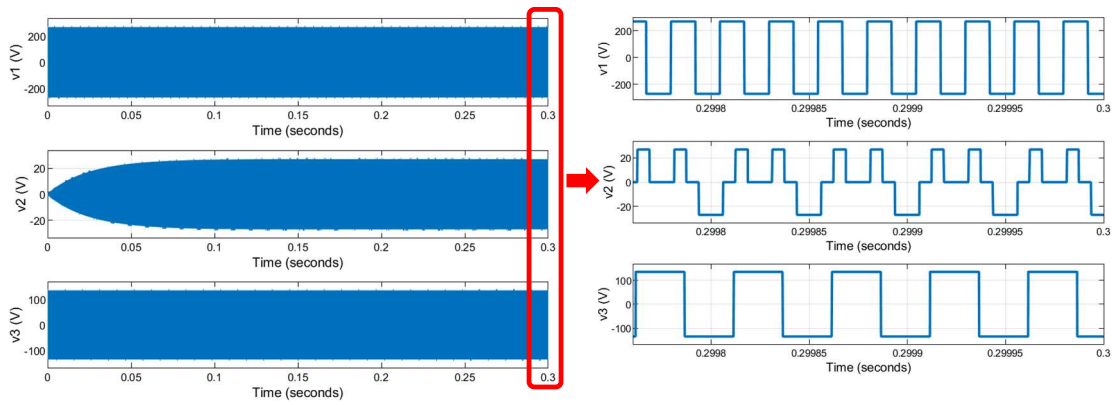
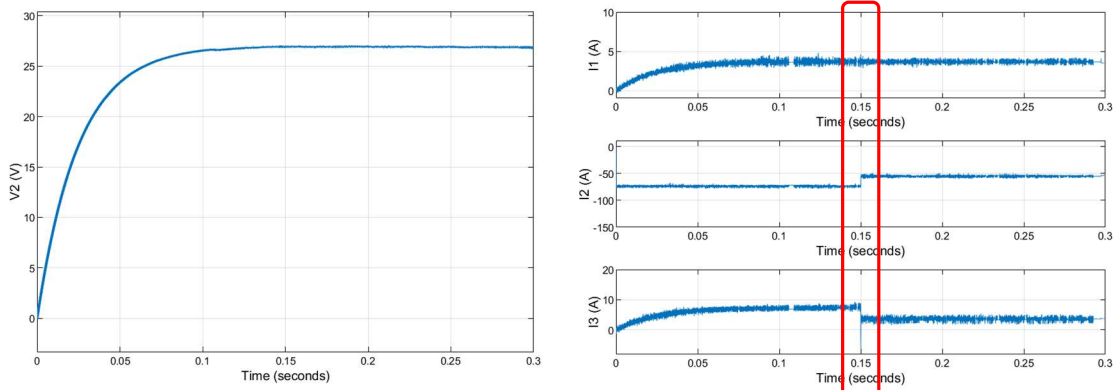


Figure 29 AC Voltages in Two Sources/ One Load



(a)

(b)

**Figure 30 Load Port 2 DC Voltage, and DC Currents in Two Sources / One Load:
(a) Resistive Load Port DC Voltage (b) DC Currents**

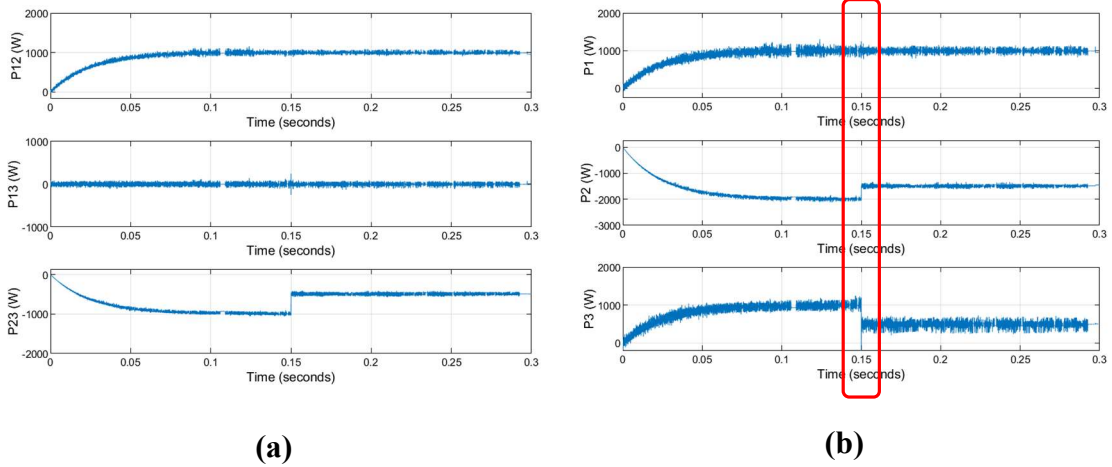


**Figure 31 Linking Transferred Power and Port Power in Two Sources/ One Load:
 (a) Linking Transferred Power (b) Port Power**

Fig. 29 shows the AC voltages in the AC link of the system. As can be seen from this figure, the voltage in the resistive load port 2 ramps up in the transient state and reaches to the expected value of 27 V in the steady-state condition. Fig. 30 shows the DC bus voltage in the resistive load port 2, and the DC currents in all ports. As can be seen from Fig. 30a, the DC voltage of the resistive load is established on 27 V after a smooth transient. According to Fig. 30b, by reducing the supplying power in the source port 3 in 0.15 S, current in port 3 is reduced, and as the result of that, there is a reduction in the load port current, proportionally. But, the point is that there is no change in the value of the current in the source port 1 after changing the current in source port 3. This shows that changing the phase shift between the source port 3 and the load port 2 does not have any effect on the supplying power in source port 1. In other words, the supplying power in the source ports can be controlled independently from each other. This is shown in Fig. 31 as well. As can be seen from Fig. 31a, by changing the supplying power in source port 3, there is

only a change in the transferred power from source port 3 to load port 2 and there is no change in the value of the transferred power between the source port 1 and the load port 2. Also, the transferred power between the source ports, P_{13} , is zero. The performance of the system can be validated by Fig. 31b as well. As can be seen from this figure, all the ports follow the expected powers, accurately both before and after the reduction in the supplying power in port 3, without any interference between the source ports.

Table. 4 shows the operation condition of the two sources/ one load system in simulation when there is a voltage drop in one of the source ports.

Table 4 Operation Condition in Simulated Two Sources/ One Load System with a Voltage Drop in One of the Source Ports

Two Sources / One Load with 25% Voltage Drop in Source Port 3			
Port No.	Port 1	Port 2	Port 3
Source/ Load	Source	Load	Source
Frequency	40 kHz	20 kHz & 40 kHz	20 kHz
DC Bus Voltage	270 V	27 V	$135 \rightarrow 135 \cdot 0.75 = 101.25 \text{ V}$
Power	1 kW	2 kW	1 kW
Phase	1.1057	1.5374	$1.3386 \rightarrow 1.2604$

As can be seen from the table, the supplying power in each one of the source ports is 1 kW and it will be kept in the same value for the entire simulation. At the time of 0.15 seconds, there is a 25% drop in the voltage of the source port 3 from 135 V to 101.25 V. In order to keep the same supplying and load powers, the phase shift between the source

port 3 and the load port must be increased, as it can be noticed in Table. 4. The simulation results for this condition are shown in Fig. (32)-(34).

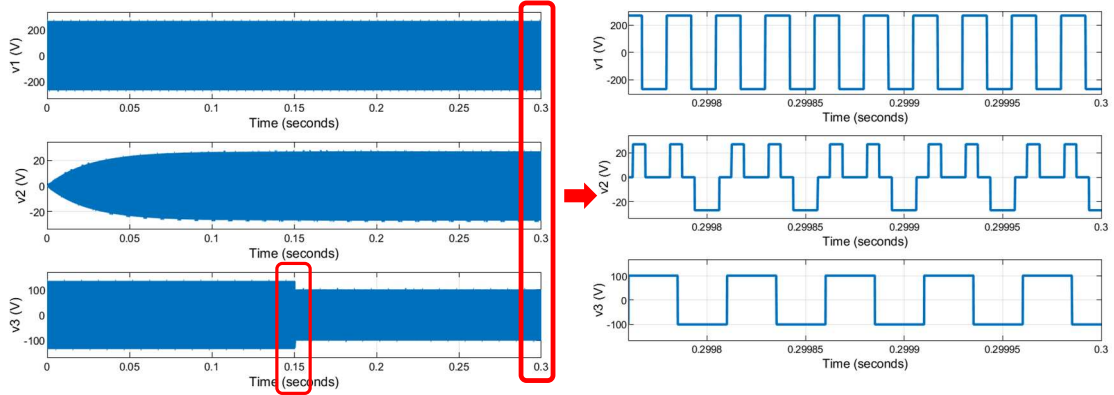


Figure 32 AC Voltages in Two Sources/ One Load with 25% Voltage Drop in Source Port 3

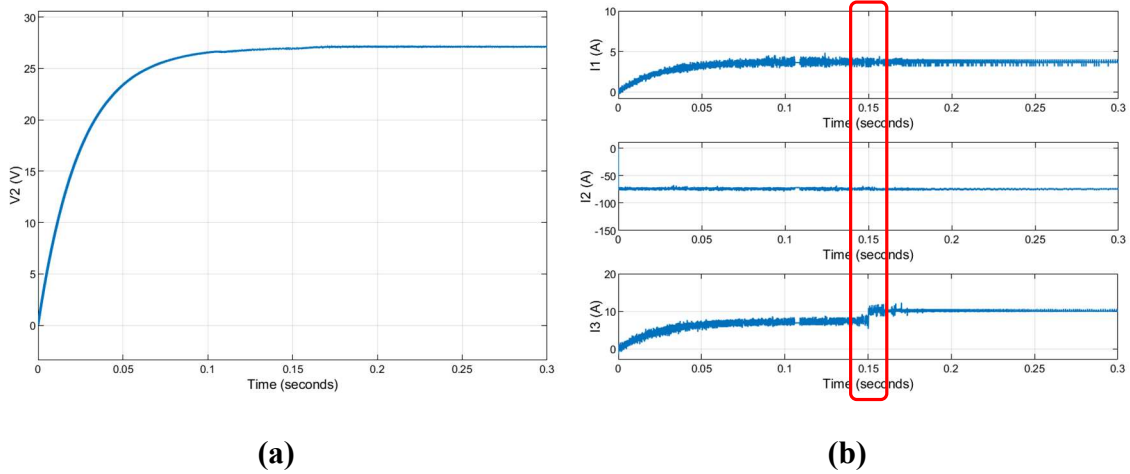


Figure 33 Load Port 2 DC Voltage, and DC Currents in Two Sources / One Load with 25% Voltage Drop in Source Port 3: (a) Resistive Load Port DC Voltage (b) DC Currents

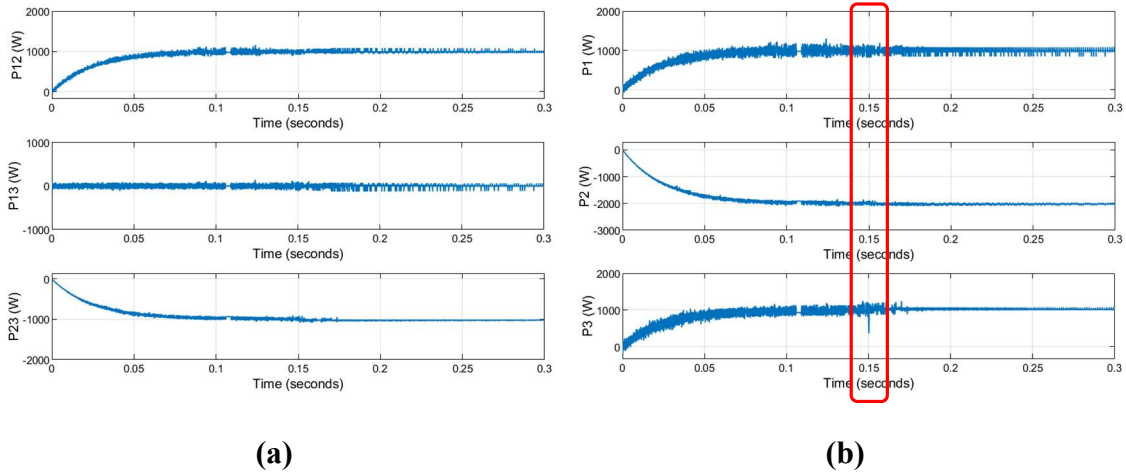


Figure 34 Linking Transferred Power and Port Power in Two Sources/ One Load with 25% Voltage Drop in Source Port 3: (a) Linking Transferred Power (b) Port Power

Fig. 32 shows the AC voltages in the AC link of the system. As can be seen from this figure, there is a drop in the value of the voltage in the source port 3 at time of 0.15 S. The effect of this reduction of the voltage can be seen from from in Fig. 33b, where the current in port 3 is increased to compensate this voltage drop and keep the same supplying power in port 3. The interesting point is that there is no change in the value of the current in the other ports after the drop in the voltage of the source port 3. This shows that changing the phase shift between the source port 3 and the load port 2 does not have any effect on the supplying power in source port 1. In other words, the supplying power in the source ports can be controlled independently from each other. This can be found from Fig. 34 as well. As can be seen from this figure, by dropping voltage in source port 3, there is no change in the value of the transferred power between the ports and also in the power of the ports. This shows that the port with the dropped voltage can regulate its power with increasing its own current without interfering other ports.

Table. 5 shows the simulation operation condition for a system with one source/ one load/ one port with zero power.

Table 5 Operation Condition in the Simulated System with One Source/ One Load/ One Port with Zero Power

One Source / One Load/ One Port with Zero Power			
Port No.	Port 1	Port 2	Port 3
Source/ Load	Source	Load	Load → Zero
Frequency	20 kHz	20 kHz	20 kHz → 40 kHz
DC Bus Voltage	270 V	27 V	135 V
Power	2 kW → 1 kW	1 kW	1 kW → 0
Phase	0	0.0961	0.0961

As can be seen from the table, at the beginning of the simulation, all ports have the frequency of 20 kHz, the demanded power in the load port 2 and load port 3 are both 1 kW, and the supplying power in the source port 1 is 2 kW. At the time of 0.15 S, there is a change in the frequency of ports 3 from 20 kHz to 40 kHz, and as the result of that the power in port 3 will drop to zero, and the power in the source port 1 is decreased to 1 kW, subsequently. The simulation results for this condition are shown in Fig. (35)-(37).

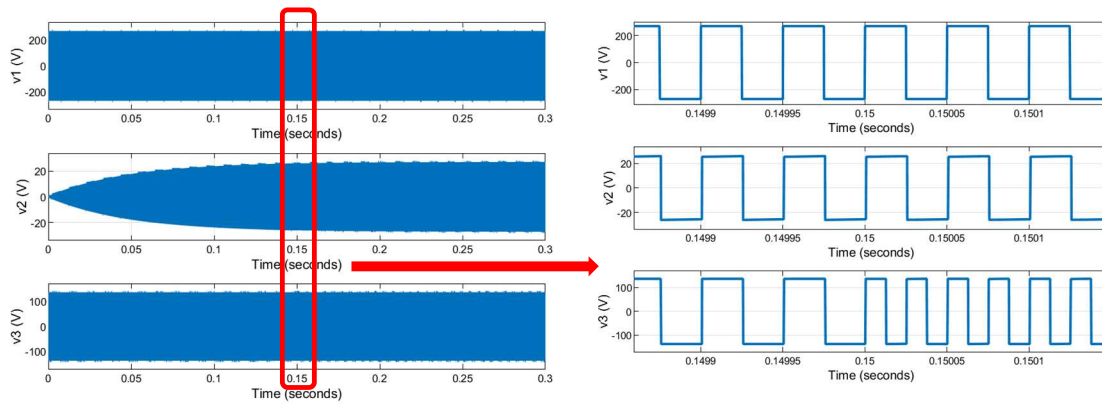


Figure 35 AC Voltages in One Source/ One Load/ One Port with Zero Power

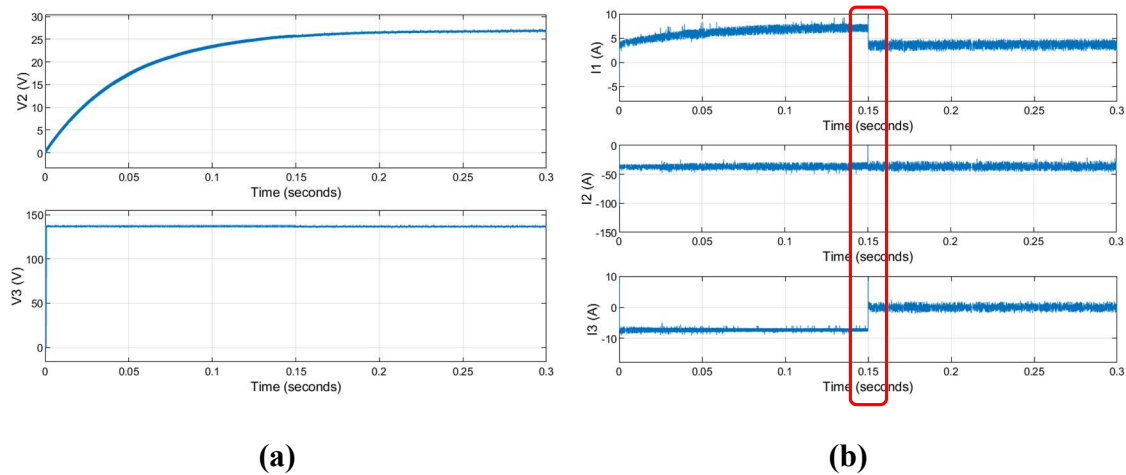


Figure 36 DC Voltages, and DC Currents in One Source/ One Load/ One Port with Zero Power: (a) Port 2 and Port 3 DC Voltage (b) DC Currents

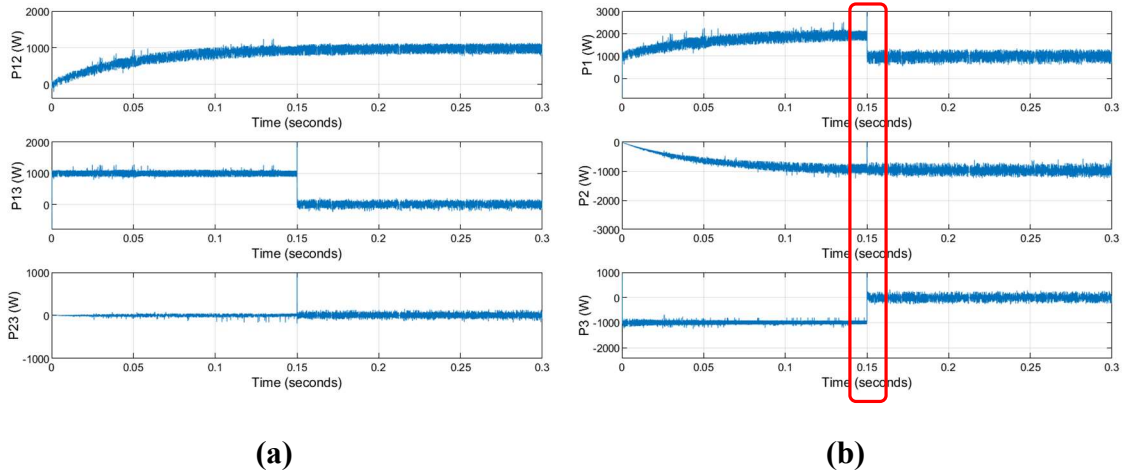


Figure 37 Linking Transferred Power and Port Power in One Source/ One Load/ One Port with Zero Power: (a) Linking Transferred Power (b) Port Power

Fig. 35 shows the AC voltages in the AC link of the system. As can be seen from this figure, the voltage in the resistive load port 2 ramps up in the transient state and reaches to the expected value of 27 V in the steady-state condition. Fig. 36 shows the DC bus voltage in the resistive load port 2, and the DC currents in all ports. As can be seen from from Fig. 36a, the DC voltage of the resistive load is established on 27 V after a smooth transient. According to Fig. 36b, by changing the frequency in port 3 at 0.15 S, the current in port 3 is dropped to zero, and the current in the source port 1 is reduced proportional to the new load power, consequently. But, the point is that there is no change in the value of the current in the load port 2 after changing the frequency in port 3. This shows that the power can be transferred selectively between each two source and load ports independently from the others. This is shown in Fig. 37 as well. As can be seen from Fig. 37a, by changing the frequency in port 3, there is no changed in the transferred power to the load port 2. The performance of the system can be validated by Fig. 37b as well. As

can be seen from this figure, all the ports follow the expected powers, accurately both before and after the transition in the frequency of port3.

Experimental Validation of Multi-Frequency Triple Active Bridge Power Conversion System

The concept of transferring power through multiple frequency channels has been validated experimentally, in this research, by a Multi-Frequency Triple Active Bridge power conversion system in the Texas A&M University Power Electronics and Motor Drives Laboratory. Fig. 38 shows a picture of the experimental setup.

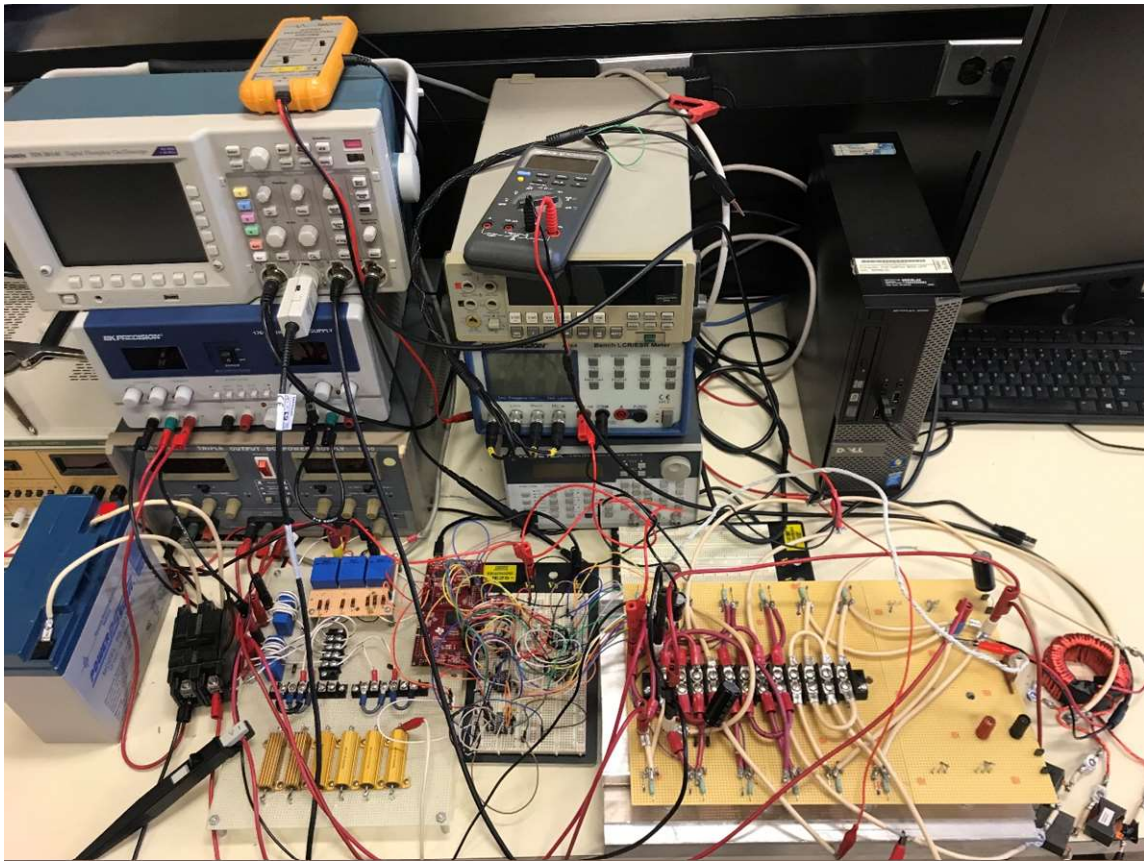


Figure 38 Multi-Frequency Triple Active Bridge Power Conversion System Experimental Setup

The experimental setup is included bellow components:

- Twelve IRFP3703PbF MOSFETs, four for each port
- One TI C2000 Delfino F28379D Microcontroller
- One high-frequency ferrite core three-winding transformer which has been built in the lab for this experiment
- Six LT 1160 Gate Driver, two for each port
- Three 3.3 μH IHDF-1300AE-10 external inductor, one for each port
- Three 6.8 mF Capacitors, one for each port
- One 12 V lead Acid Battery
- Voltage and current sensors, resistive loads, and instruments like DC power supply, oscilloscope, digital multi meter, RLC meter, differential probe etc.

The measured leakage inductance of the transformer is 0.4 μH for each port and, therefore, the total inductance including the external ones is 3.7 μH for each port.

Totally five experiments have been run for the proof-of-concept validation of the experimental setup. Here is the summary of the experiments:

- One Source/ Two Loads with balanced loads
- One Source/ Two Loads with unbalanced loads
- Two Sources/ One Load with equal source voltages
- Two Sources/ One Load with a voltage drop in one of the sources
- One Source/ One Load/ One Port with Zero Power

The results of the experiments are shown in Fig. (39)-(44).

Table. 6 shows the experiment condition for the one source/ two loads case with balanced loads, and Fig. 39 shows the results of the experiment.

Table 6 Experiment Condition for One Source/ Two Loads with Balanced Loads

One Source/ Two Loads with Balanced Loads			
Port No.	Port 1	Port 2	Port 3
Source/ Load	Source (DC Power Supply)	Load (Resistor)	Load (Resistor)
Frequency	20 kHz & 40 kHz	40 kHz	20 kHz
DC Bus Voltage	16 V	8 V	8 V
Power	12.8 W	6.4 W	6.4 W

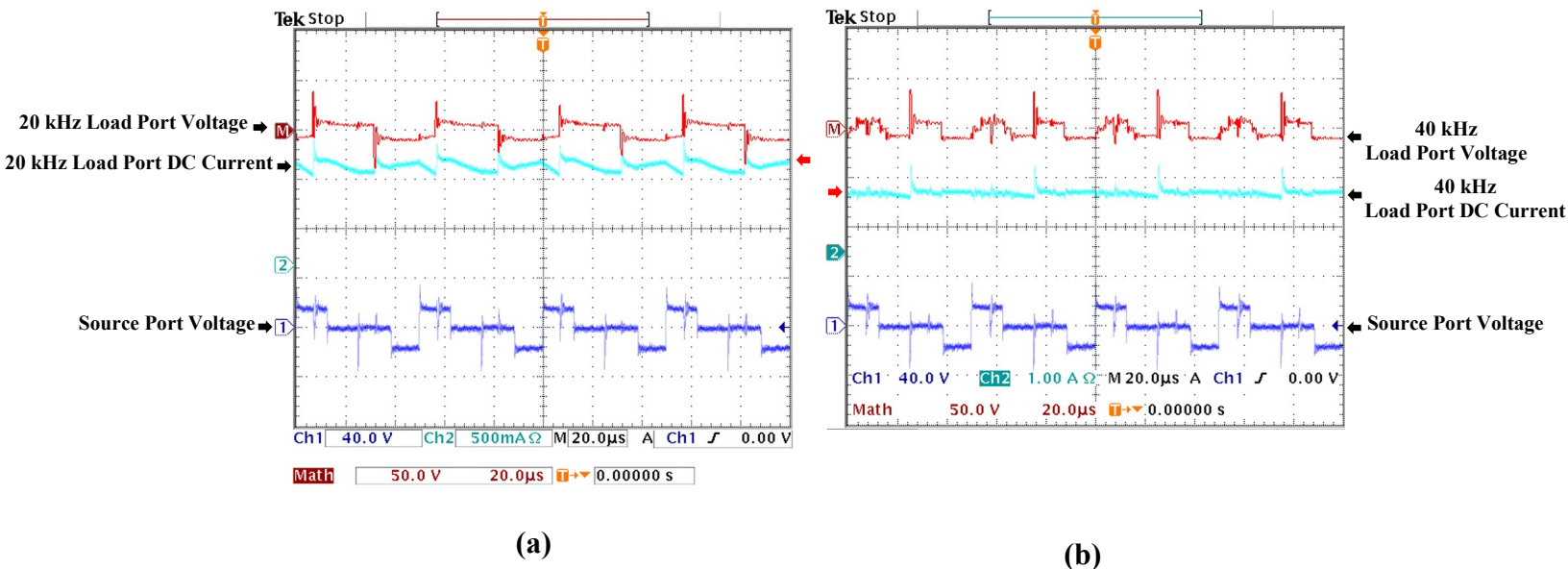


Figure 39 Experimental Results for One Source/ Two Loads with Balanced Loads

The red color is for the AC voltage of the load port with the frequency of 20 kHz in Fig. 39a, and the AC voltage of the load port with the frequency of 40 kHz in Fig. 39b. The cyan color is for the DC current of the load port with the frequency of 20 kHz in Fig. 39a, and the DC current of the load port with the frequency of 40 kHz in Fig. 39b. The blue color is for the AC voltage of the source port with the frequency of 20 kHz & 40 kHz. As can be seen from the figure, the averaged current in both load ports is around 0.8 A which is matched with the power and the voltage in these ports.

Table. 7 shows the experiment condition for the one source/ two loads case with balanced loads, and Fig. 40 shows the results of the experiment.

Table 7 Experiment Condition for One Source/ Two Loads with Unbalanced Loads

One Source/ Two Loads with unbalanced Loads			
Port No.	Port 1	Port 2	Port 3
Source/ Load	Source (DC Power Supply)	Load (Resistor)	Load (Resistor)
Frequency	20 kHz & 40 kHz	40 kHz	20 kHz
DC Bus Voltage	16 V	8 V	8 V
Power	14.9 W	6.4 W	8.5 W

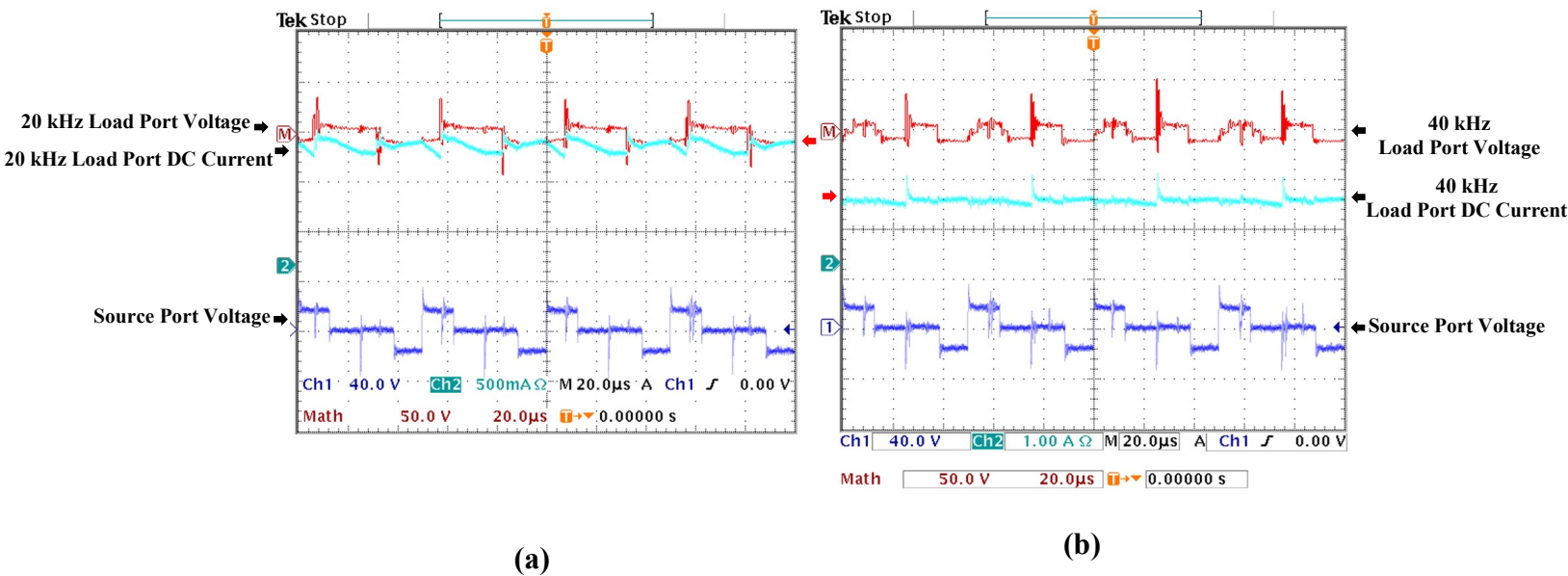


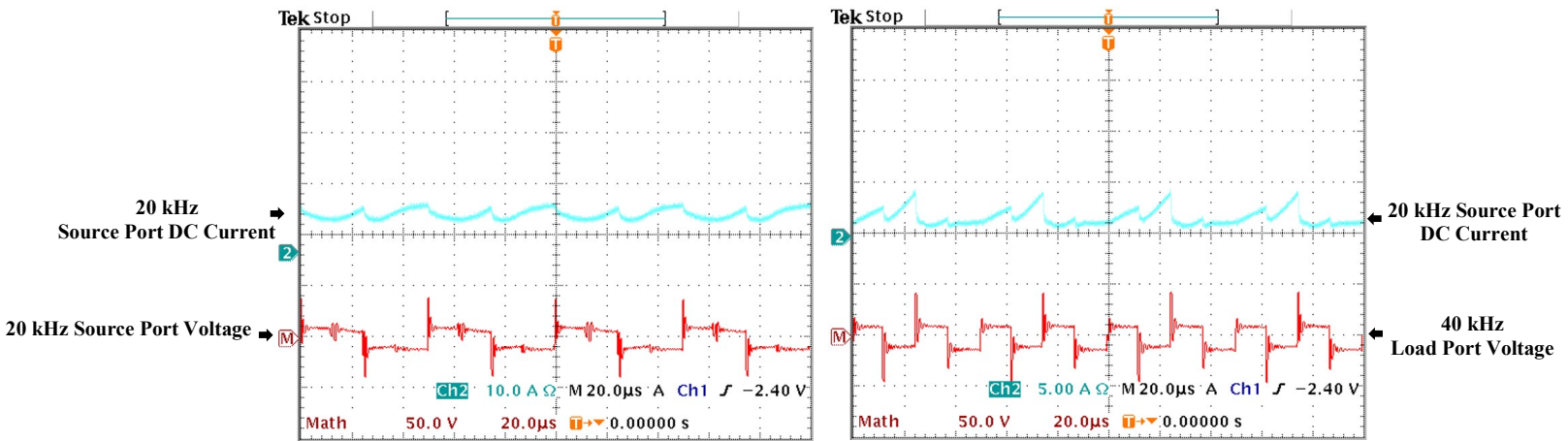
Figure 40 Experimental Results for One Source/ Two Loads with Unbalanced Loads

In this experiment, the power in the load port with the frequency of 20 kHz is increased to 8.5 W and, as the result of that, the averaged current in this port is increased to around 1 A, as it is shown in Fig. 40a. The interesting point is that with this increase in the current in the port with the frequency of 20 kHz there is no change in the value of current in the port with frequency of 40 kHz. As can be seen from Fig. 40b, the averaged current in the port with the frequency of 40 kHz is kept on around 0.8 A which is same as its value in the balanced case. This shows that the power in the port with the frequency of 20 kHz can be controlled independently from the with the frequency of 40 kHz.

Table. 8 shows the experiment condition for the two sources/ one load case with equal source voltages, and load power of 28.8 W. Fig. 41 shows the results of this experiment.

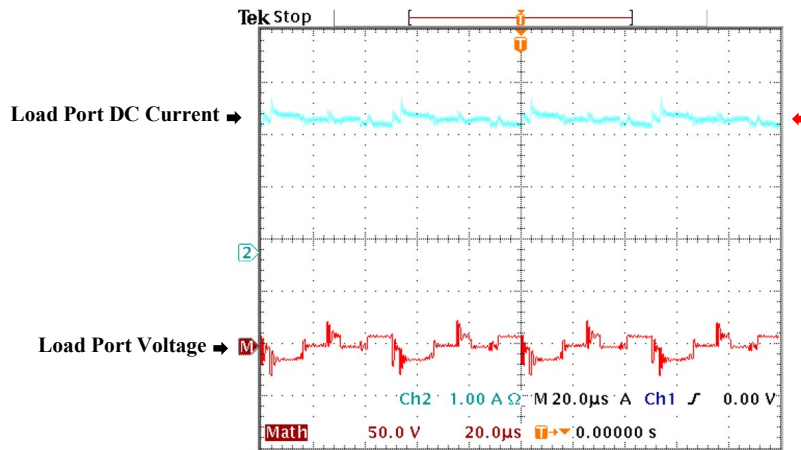
Table 8 Experiment Condition for Two Sources/ One Load

Two Sources/ One Load with Equal Source Voltages and Load Power of 28.8 W			
Port No.	Port 1	Port 2	Port 3
Source/ Load	Source (DC Power Supply)	Load (Resistor)	Source (Battery)
Frequency	40 kHz	20 kHz & 40 kHz	20 kHz
DC Bus Voltage	12 V	12 V	12 V



(a)

(b)



(c)

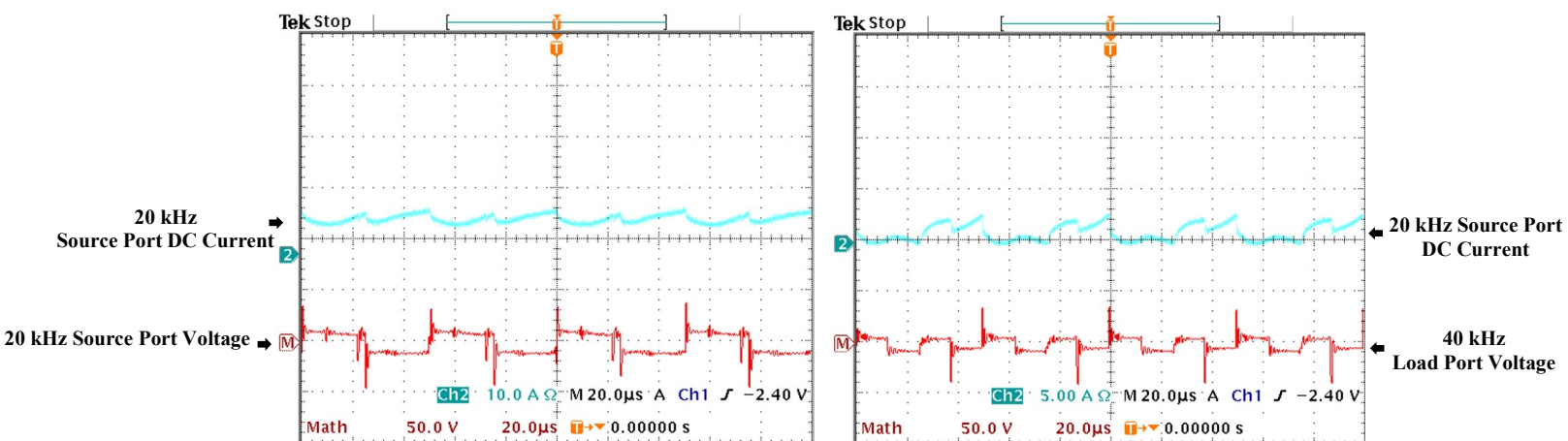
Figure 41 Experimental Results for Two Sources/ One Load

The red color is for the AC voltage of the source port with the frequency of 20 kHz in Fig. 41a, the AC voltage of the source port with the frequency of 40 kHz in Fig. 41b, and the AC voltage of the load port with the frequency of 20 kHz & 40 kHz in Fig. 41c. The cyan color is for the DC current of the source port with the frequency of 20 kHz in Fig. 41a, the DC current of the source port with the frequency of 40 kHz in Fig. 41b, and the DC current of the load port with the frequency of 20 kHz & 40 kHz in Fig. 41c. As can be seen from Fig. 41c, the averaged current in load port is 2.4 A which is matched with the power and the voltage of the port.

Table. 9 shows the experiment condition for the two sources/ one load case with 50% drop in the source port with the frequency of 40 kHz, and the load power of 19.2 W. Fig. 42 shows the results of this experiment.

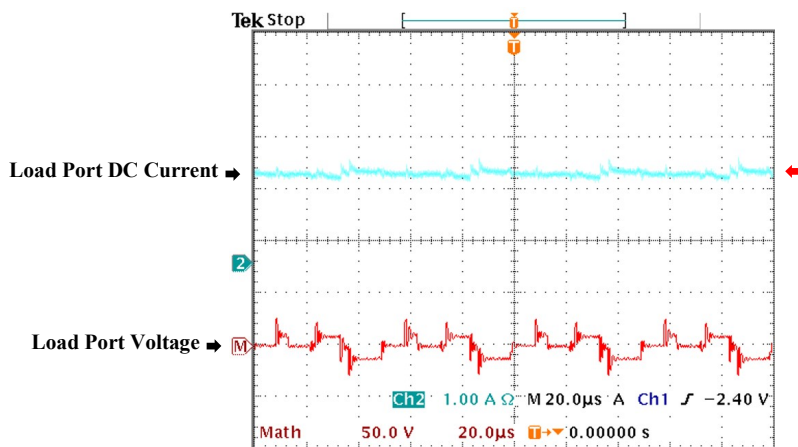
Table 9 Experiment Condition for Two Sources/ One Load with Voltage Drop in One Source

Two Sources/ One Load with Voltage Drop in One Source and Load Power of 19.2 W			
Port No.	Port 1	Port 2	Port 3
Source/ Load	Source (DC Power Supply)	Load (Resistor)	Source (Battery)
Frequency	40 kHz	20 kHz & 40 kHz	20 kHz
DC Bus Voltage	6 V	12 V	12 V



(a)

(b)



(c)

Figure 42 Experimental Results for Two Sources/ One Load with Voltage Drop in One Source and Load Power of 19.2 W

As can be seen from Fig. 41c, in comparison to Fig. 40c, the averaged current in load port is decreased to 1.6 A with the drop in the source voltage in the port with the frequency of 40 kHz. This reduction in the voltage in the source port with the frequency of 40 kHz and in the power of the load port does not have any effect on the source port with the frequency of 20 kHz. This means an independent power flow control between the sources and load.

Table. 10 shows the experiment condition for the two sources/ one load/ one port with zero power case with the load power of 14.4 W. Fig. 43 shows the results of this experiment.

Table 10 Experiment Condition for One Sources/ One Load/ One Port with Zero Power

One Sources/ One Load/ One Port with Zero Power with the Load Power of 14.4 W			
Port No.	Port 1	Port 2	Port 3
Source/ Load	Source (DC Power Supply)	Load (Resistor)	Zero (Resistor)
Frequency	20 kHz	20 kHz	40 kHz
DC Bus Voltage	12 V	12 V	-

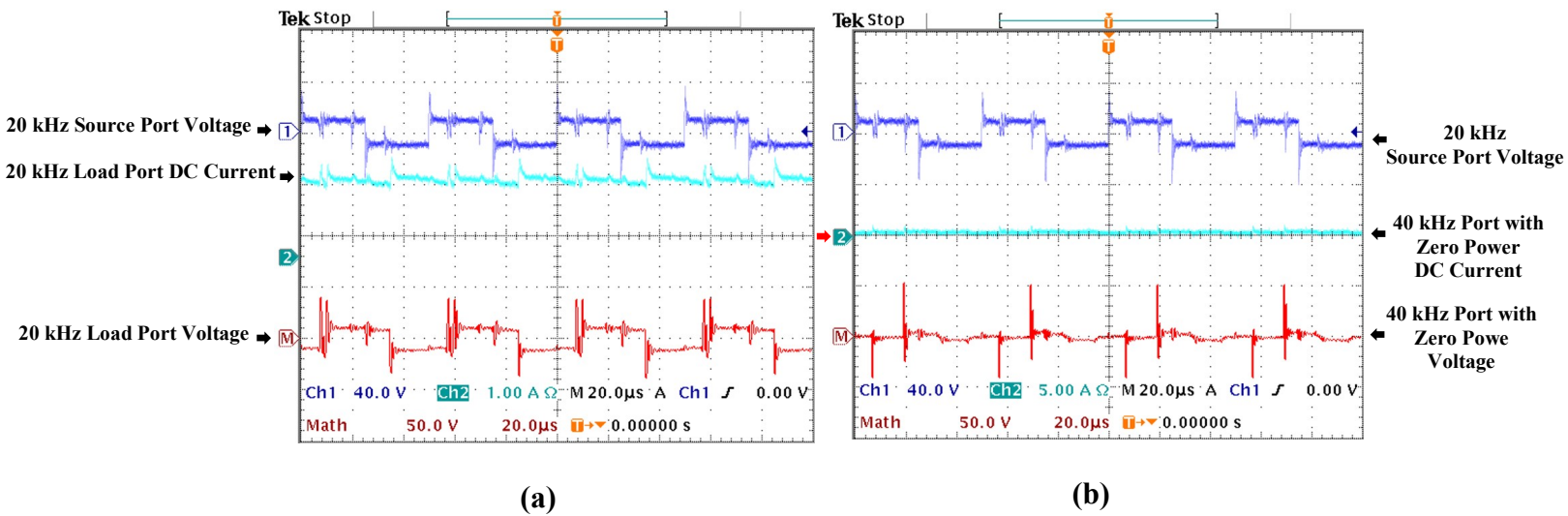


Figure 43 Experimental Results for One Source/ One Load/ One Port with Zero Power

The red color is for the AC voltage of the load port with the frequency of 20 kHz in Fig. 43a, and the AC voltage of the port with zero power and the frequency of 40 kHz in Fig.

43b. The cyan color is for the DC current of the load port with the frequency of 20 kHz in Fig. 43a, and the DC current of the port with zero power and the frequency of 40 kHz in Fig. 43b. The blue color is for the AC voltage of the source port with the frequency of 20 kHz. As can be seen from Fig. 43a, the DC current in the load port with the frequency of 20 kHz is 1.2 A which is matched with the power and the voltage in this port. The interesting point is that the DC current in the port with the frequency of 40 kHz is zero which means a zero power in this port. Since the port with the frequency of 40 kHz is a resistive port and because of having zero DC current in this port, the voltage of the port cannot be established to the reference value of the controller, and as the result, the value of the DC bus voltage in this port is approximately zero.

CHAPTER VII

CONCLUSION

In this research, a novel power electronics-based power distribution system is introduced, which creates the possibility of adding virtual frequency channels to the power system each one of these channels is inherently isolated. The frequency channels will not interfere with each other due to orthogonality of the waveforms. All the harmonic frequencies from the power electronics converters are included in the system, and because of that, the frequency channels are completely decoupled, and power can be transferred between every combination of the sources and loads, independently through isolated frequency channels, without interfering the others. The proposed system is based on a multi-frequency multiport power conversion system in which power is integrated at various frequencies at the source ends and selectively picked up by the loads, or vice versa.

After analyzing power transfer in multiport power conversion systems, interactions between the ports is recognized as the main challenge of the system which limits the flexibility of power flow management between any selected combination of the sources and loads. This issue gets more challenging when there are unbalanced load demands, different source voltages, limitations in supplying power one or more ports, faults in one or more ports, different linking inductance values, or when there are series or parallel connections between the ports. To address this issue for a system with any number of ports, and to transfer power selectively between any combination of the ports with any source voltages or demanded load powers, a solution is proposed in this research. That is,

creating virtual isolated frequency channels between each two ports of the system so that the power can be transferred completely independently through each frequency channel without interfering the others.

The concept of transferring power through different frequencies has been investigated in this research. As the result, it has been found that in order to have independent frequency channels between the ports in a multiport power conversion system, the frequency of the channels must be an even coefficient of the reference frequency without an odd factor, which the reference frequency must be determined according to the design requirements. Having investigated the concept of transferring power through independent frequency channels, the concept of multi-frequency multiport power conversion systems has been discussed then, and different modes of operation of the system and the averaged transferred power in each mode has been analyzed.

To realize the concept of multi-frequency power transfer in multiport power conversion systems, a Multi-Frequency Multi Active Bridge power conversion system has been introduced in this research in which the isolated frequency channels are created by assigning different frequencies to the legs of the active bridges in the system. Different modes of transferring power have been investigated in Multi-Frequency Multi Active Bridge power conversion systems, and the averaged transferred power expressions have been derived in each mode.

For the proof-of-concept validation, a Multi-Frequency Triple Active Bridge power conversion system including a power management module and voltage and current control loops has been implemented by both simulation and experiment. The performance of the

system has been validated in transient and static states for one source/ two loads, two sources/ one load, and one source/ one load/ one port with zero power conditions. As the result, it has been shown that:

- The demanded power in the load ports in the one source/ two loads condition can be controlled independently in each load even in the unbalanced load condition
- The supplying power in the source ports in the two sources/ one load condition can be controlled independently in each source even with a voltage drop in one of the sources
- The power in the one source/ one load/ one port with zero power condition can be transferred flexibly between each two selected source and load ports without interchanging power with the third one

REFERENCES

- [1] H. Matsuo, W. Lin, F. Kurokawa, T. Shigemizu, and N. Watanabe, "Characteristics of the Multiple-Input DC–DC Converter," *IEEE Transactions on Industrial Electronics*, Vol. 51, No. 3, June 2004.
- [2] A. Maina Ari, L. Li, and O. Wasynczuk, "Control and Optimization of N-Port DC–DC Converters," *IEEE Transactions on Control Systems Technology*, Vol. 24, No. 4, July 2016.
- [3] S. Falcones, R. Ayyanar and X. Mao, "A DC–DC Multiport-Converter-Based Solid State Transformer Integrating Distributed Generation and Storage," *IEEE Transactions on Power Electronics*, Vol. 28, No. 5, May 2013.
- [4] B. Karanayil, M. Ciobotaru, and V. G. Agelidis, "Power Flow Management of Isolated Multiport Converter for More Electric Aircraft," *IEEE Transactions on Power Electronics*, Vol. 32, No. 7, July 2017.
- [5] G. Buticchi, L. F. Costa, D. Barater, M. Liserre, and E. D. Amarillo, "A Quadruple Active Bridge Converter for the Storage Integration on the More Electric Aircraft," *IEEE Transactions on Power Electronics*, Vol. 33, No. 9, September 2018.
- [6] L. F. Costa, G. Buticchi, and M. Liserre, "Quad-Active-Bridge DC–DC Converter as Cross-Link for Medium-Voltage Modular Inverters," *IEEE Transactions on Industry Applications*, Vol. 53, No. 2, March/April 2017.

- [7] C. Gu, Z. Zheng, L. Xu, K. Wang, and Y. Li, "Modeling and Control of a Multiport Power Electronic Transformer (PET) for Electric Traction Applications," *IEEE Transactions on Power Electronics*, Vol. 31, No. 2, February 2016.
- [8] H. Tao, A. Kotsopoulos, J. L. Duarte, and M. A. M. Hendrix, "Transformer-Coupled Multiport ZVS Bidirectional DC–DC Converter with Wide Input Range," *IEEE Transactions on Power Electronics*, Vol. 23, No. 2, March 2008.
- [9] J. L. Duarte, M. Hendrix, and M. G. Simões, "Three-Port Bidirectional Converter for Hybrid Fuel Cell Systems," *IEEE Transactions on Power Electronics*, Vol. 22, No. 2, March 2007.
- [10] L. Ortega, P. Zumel, C. Fernández, J. López-López, A. Lázaro, and A. Barrado, "Power Distribution Algorithm and Steady-State Operation Analysis of a Modular Multiactive Bridge Converter," *IEEE Transactions on Transportation Electrification*, Vol. 6, No. 3, September 2020.
- [11] L. F. Costa, G. Buticchi, and Marco Liserre, "Optimum Design of a Multiple-Active-Bridge DC–DC Converter for Smart Transformer," *IEEE Transactions on Power Electronics*, Vol. 33, No. 12, December 2018.
- [12] L. F. Costa, F. Hoffmann, G. Buticchi, and M. Liserre, "Comparative Analysis of Multiple Active Bridge Converters Configurations in Modular Smart Transformer," *IEEE Transactions on Industrial Electronics*, Vol. 66, No. 1, January 2019.

- [13] Y. Chen, P. Wang, Y. Elasser, and M. Chen, "Multicell Reconfigurable Multi-Input Multi-Output Energy Router Architecture," *IEEE Transactions on Power Electronics*, Vol. 35, No. 12, December 2020.
- [14] V. N. S. R. Jakka, A. Shukla, and G. D. Demetriades, "Dual-Transformer-Based Asymmetrical Triple-Port Active Bridge (DT-ATAB) Isolated DC–DC Converter," *IEEE Transactions on Industrial Electronics*, Vol. 64, No. 6, June 2017.
- [15] E. S. Oluwasogo, and H. Cha, "Self-Current Sharing in Dual-Transformer-Based Triple-Port Active Bridge DC-DC Converter with Reduced Device Count," *IEEE Transactions on Power Electronics*, 2020.
- [16] V. N. S. R. Jakka, A. Shukla, and S. V. Kulkarni, "Flexible Power Electronic Converters for Producing AC Superimposed DC (ACsDC) Voltages," *Transactions on Industrial Electronics*, Vol. 65, No. 4, April 2018.
- [17] R. Y. Barazarte Conte, "Investigation of Multi-Frequency Power Transmission and System," *Texas A&M University August 2011*.
- [18] J. A. Ferreira, "The Multilevel Modular DC Converter," *Transactions on Power Electronics*, Vol. 28, No. 10, October 2013.
- [19] S. Bruske, G. Buticchi, and M. Liserre, "Multifrequency Single-Phase Islanded Grids," *Transactions on Industrial Electronics*, Vol. 65, No. 12, December 2018.
- [20] M. H. Kheraluwala, R. W. Gascoigne, D. M. Divan, and E. D. Baumann "Performance Charactrisation of a High-Power Dual Active Bridge dc-to-dc Converter," *IEEE Transaction on Industry Applications*, Vol. 28, No. 6, November/ December 1992.

- [21] B. Rahrovi, M. Ehsani, "A Review of the More Electric Aircraft Power Electronics," *IEEE Texas Power and Energy Conference, 2019*.
- [22] R. Sabzehgar, "A Review of AC/DC Microgrid–Developments, Technologies, and Challenges," *IEEE 2015*.
- [23] P. Ghimire, D. Park, M. Karbalaye Zadeh, J. Thorstensen, and E. Pedersen, "Shipboard Electric Power Conversion: System Architecture, Applications, Control, and Challenges," *IEEE Electrification Magazine, December 2019*.
- [24] G. R. Chandra Mouli1, P. Bauer, and M. Zeman, "Comparison of System Architecture and Converter Topology for a Solar Powered Electric Vehicle Charging Station," *International Conference on Power Electronics, June 2015*.
- [25] F. Krismer, "Modeling and Optimization of Bidirectional Dual Active Bridge DC–DC Converter Topologies," *ETH Zurich, 2010*.
- [26] B. Rahrovi, R. Tafazzoli Mehrjardi, M. Ehsani, "On the Analysis and Design of High-Frequency Transformers for Dual and Triple Active Bridge Converters in More Electric Aircraft," *IEEE Texas Power and Energy Conference, 2021*.